# Competing targets of microRNA-608 affect anxiety and hypertension

Geifman-Shochat, Susana; Hanin, Geula; Shenhar-Tsarfaty, Shani; Yayon, Nadav; Hoe, Yau Yin; Bennett, Estelle R.; Sklan, Ella H.; Rao, Dabeeru. C.; Rankinen, Tuomo; Bouchard, Claude; Shifman, Sagiv; Greenberg, David S.; Soreq, Hermona

2014

Hanin, G., Shenhar-Tsarfaty, S., Yayon, N., Hoe, Y. Y., Bennett, E. R., Sklan, E. H., et al. (2014). Competing targets of microRNA-608 affect anxiety and hypertension. Human Molecular Genetics, in press.

https://hdl.handle.net/10356/103870

https://doi.org/10.1093/hmg/ddu170

# Competing targets of microRNA-608 affect anxiety and hypertension

| | |
|---|---|
| Journal: | *Human Molecular Genetics* |
| Manuscript ID: | HMG-2014-D-00056.R1 |
| Manuscript Type: | 2 General Article - UK Office |
| Date Submitted by the Author: | 04-Mar-2014 |
| Complete List of Authors: | Hanin, Geula; The Hebrew University of Jerusalem, Biological Chemistry<br>Shenhar-Tsarfaty, Shani; The Hebrew University of Jerusalem, Biological Chemistry<br>Yayon, Nadav; The Hebrew University of Jerusalem, Biological Chemistry<br>Yin Hoe, Yau; Nanyang Technological University, Biological Sciences<br>Bennett, Estelle; The Hebrew University of Jerusalem, Biological Chemistry<br>Sklan, Ella; Tel Aviv University, Clinical Microbiology and Immunology<br>Rao, Dabeeru C.; Dept. of Biostatistics, Washington University, Box 8067<br>Rankinen, Tuomo; PBRC, Human Genomics<br>Bouchard, Claude; Pennington Biomedical Research Center, Human Genomics Laboratory<br>Geifman-Shochat, Susana; Nanyang Technological University, Biological Sciences<br>Shifman, Sagiv; The Hebrew University of Jerusalem, Genetics<br>Greenberg, David; The Hebrew University of Jerusalem, Biological Chemistry<br>Soreq, Hermona; The Hebrew University of Jerusalem, Biological Chemistry |
| Key Words: | miRNA, Acetylcholinesterase, SNP, anxiety, hypertension |
| | |

Dear Prof. Davies,

Thank you for the constructive review of our manuscript.
We found the reviewers' comments both informative and important, performed much additional work and revised our manuscript accordingly. A new figure has been added, and the text was revised as well. We thank the reviewers for addressing the weakness points in this study and made an effort to strengthen these points as recommended. In addition, we prepared a suggested cover image for this article which has also been submitted. Please see below our detailed point-by-point answers to the reviewers' comments.

All formatting errors found in the manuscript were corrected according to the instructions.

We are particularly grateful to reviewer no. 2 for his/her in-depth review, and for the satisfaction with our experimental design and technical performance.

Reviewer no. 1 commented:

"In HEK293T cells there is a 3-fold repression of the luciferase reporter by miR-608 (Fig 1F), whereas a minor effect is observed at the level of AChE activity in U937 cells. What happens at the AChE protein levels in U937 cells? "

We found this comment important and performed an immunoblot analysis for the AChE protein in U937 cells exposed to miR-608 compared to controls. A robust effect was observed at the level of the AChE protein, and, as we previously showed, this effect was considerably larger than that observed in the catalytic activity of the AChE enzyme, compatible with a large fraction of the AChE protein being catalytically inactive (as we previously reported in Shaked et al. Immunity 2009). Fig 1G in the manuscript had been revised accordingly, demonstrating a similarly robust suppression of the AChE protein by miR-132 and miR-608.

"The authors argue that the reduced interaction between miR-608 and AChE in the presence of the minor allele potentiates the repression of other miR-608 targets. However the Western-blot shown in Fig. 3B does not corroborate this conclusion/claim. "

To refine the presentation we replaced the presented blot with a more representative one. We hope that the outcome of greater difference between the control and the miR-608 treated cells for the major and minor alleles will be clearer in this revised figure.

"Moreover, for the in vitro experiments the authors restrict their analysis to CDC42 (Fig 3B and C), while arguing for the same effect in other targets (e.g. IL-6). It is essential to check the effect for additional miR-608 targets. Along this line, it would be most interesting to use a genome-wide approach to look at the overall targets of miR-608."

We found this comment of utmost importance for understanding the complexity aspect of miR-608 effects. To address this issue more globally, we used the miRwalk database (http://www.umm.uni-heidelberg.de/apps/zmf/mirwalk/) to identify the top 30 predicted targets of miR-608, searched for those targets that are expressed in HEK293T cells (which incidentally do not express IL6) and designed RT-PCR primers for all of these predicted targets(Supplementary Table 2). We then performed a microfluidics dynamic array experiment (Fluidigm http://www.fluidigm.com/biomark-

hd-system.html) to simultaneously quantify the levels of all of those predicted targets in cells carrying the major and minor alleles of the AChE 3'-UTR and treated with increasing doses of miR-608. Among those, we identified 3 genes (NACC1, mapped to Chr 19p13.2, with 7 putative binding sites for miR-608; TPP1, mapped to Chr 11p15, with 2 binding sites; and the validated target CD44, mapped to Chr 11p13, with one binding site) that showed similar behavior to that of CDC42 mapped to Ch 1p36.1 and IL6 mapped to Chr 7p15.3, suppression of both of which we show in human post-mortem cortices). Briefly, all of these transcripts showed dose-dependent suppression by miR-608 and cells carrying the minor A-allele presented potentiated suppression of these targets compared to those carrying the major C-allele. Thus, we have now showed that the studied SNP in the AChE gene caused allele-specific difference between the capacity of miR-608 to suppress its other targets; that this effect is not limited to CDC42 and IL6, that it does not depend on the number of miR-608 binding sites in those other targets and that it is evident in at least 4 different chromosomes. These new observations were now added to the text under Results; the quantification is presented in the revised Figure 3 (as Figure 3D), and the remaining part of Fig3 became the new Fig4, with the other figures re-numbered successively. We also added the Fluidigm procedure to the revised Methods and referred to the implications of these measurements under Discussion.

"In the experiments shown in Fig 3B and 3C, AChE 3'UTR reporter constructs containing the major allele and minor allele were introduced in HEK293T cells. How do the levels of these reporter constructs compare with the levels of AChE in cell types expressing AChE? It would be more informative to perform these experiments in a cellular model that expresses AChE and use the same background to construct minor allele mutant. "

We accept this comment; however, AChE expression levels are rather low in most cell types excluding mature differentiated brain neurons and erythrocytes, to an extent that would jeopardize measurements of expression in cells carrying the different alleles. Given this difficulty, we selected HEK293T cells that do not express endogenous AChE, which reduces the background signal to extremely low levels, and transfected them with parallel levels of the major and minor allele 3'-UTR constructs. To check the effect in those cell types expressing the native AChE alleles we interrogated post-mortem tissue samples removed from the human brain, where we could genotype the AChE alleles, determine AChE activity in the native tissue and quantify CDC42 and IL6 levels.

" The Western-blots shown in Fig 3H for CDC42 and IL6 should be improved, so that reliable quantifications can be obtained (Fig 3I and IJ). In addition it would be important to show the protein levels of AChE in these samples. "

The presentation of the IL6 western blot has been improved, and is now presented in the new Figure 4E. The protein levels of AChE were tested in HEK293T cells (revised Figure 1).

"Color legend is missing for Fig 4."

We added the color legend to the figure.

We would like to thank reviewer no. 1 again for these important comments, and believe that the introduced changes (highlighted in yellow throughout the text) improved the quality of our article.

Sincerely,

Hermona Soreq, PhD
Professor of Molecular Neuroscience
The Edmond and Lily Safra center for Brain Sciences
The Hebrew University of Jerusalem
The Edmond J. Safra Campus, Givat Ram
Jerusalem 91904 ISRAEL
Tel No: 972-2-6585109
Fax No: 972-2-6520258
Email: hermona.soreq@mail.huji.ac.il

# Competing targets of microRNA-608 affect anxiety and hypertension.

Geula Hanin[a], Shani Shenhar-Tsarfaty[a], Nadav Yayon[a], Yau Yin Hoe[b], Estelle R. Bennett[a], Ella H. Sklan[c], D. C. Rao[d], Tuomo Rankinen[e], Claude Bouchard[e], Susana Geifman-Shochat[b], Sagiv Shifman[a], David S. Greenberg[a], and Hermona Soreq[a*]

[a] The Silberman Institute of Life Sciences, The Hebrew University of Jerusalem, Givat Ram, Jerusalem 91904, Israel, and The Edmond and Lily Safra Center for Brain Science.

[b] School of Biological Sciences, Nanyang Technological University, 60 Nanyang Avenue, Singapore 637551

[c] Department of Clinical Microbiology and Immunology, Sackler School of Medicine, Tel Aviv University, Tel Aviv 69978, Israel,

[d] Division of Biostatistics, School of Medicine, Washington University in St. Louis, St. Louis, MO, USA.

[e] Human Genomics Laboratory, Pennington Biomedical Research Center, Baton Rouge, LA, USA

*To whom correspondence should be addressed: Prof. Hermona Soreq, The Edmond and Lily Safra Center for Brain Sciences, The Hebrew University of Jerusalem, The Edmond Safra Campus, Givat Ram, Jerusalem 91904, Israel. Tel: 972-2-658-5109; Fax: 972-2-652-0258 E-mail: hermona.soreq@mail.huji.ac.il.



## Abstract

MicroRNAs (miRNAs) can repress multiple targets, but how a single de-balanced interaction affects others remained unclear. We found that changing a single miRNA-target interaction can simultaneously affect multiple other miRNA-target interactions, and modify physiological phenotype. We show that miR-608 targets acetylcholinesterase (AChE) and demonstrate weakened miR-608 interaction with the rs17228616 AChE allele having a single nucleotide polymorphism (SNP) in the 3'-untranslated region (3'UTR). In cultured cells, this weakened interaction potentiated miR-608-mediated suppression of other targets, CDC42 and interleukin-6 (IL6).Post-mortem human cortices homozygote for the minor rs17228616 allele showed AChE elevation and CDC42/IL6 decreases compared to major allele homozygotes. Additionally, minor allele heterozygote and homozygote subjects showed reduced cortisol and elevated blood pressure, predicting risk of anxiety and hypertension. Parallel suppression of the conserved brain CDC42 activity by intracerebroventricular ML141 injection caused acute anxiety in mice. We demonstrate that single SNPs in miRNA-binding regions could cause expanded downstream effects changing important biological pathways.

## Introduction

MiRNAs are short non-coding RNAs, 20-25 nucleotides long, that can simultaneously regulate multiple genes in biological pathways(1) by post-transcriptionally suppressing translation and/or inducing degradation of their mRNA targets(1-3), suggesting that they are particularly suitable for controlling the rapidly adjustable physiology of the parasympathetic system. Moreover, due to the multileveled activities of Acetylcholine (ACh) signaling, miRNAs could modulate both the neuronal and immune functions of ACh by controlling its production and elimination(4, 5). However, the biological impact of maintaining multiple miRNA-target interactions balanced, the inherited diversity of miRNA regulation or how

impairments in one interaction would affect the others has not been thoroughly addressed(5).

SNP interference with miRNA functions affects the expression of corresponding targets, modifies brain functions and induces a risk of disease. In Tourette's syndrome, a 3'-UTR SNP in the brain-expressed human Slit and Trk-like-1 (SLITRK1) gene strengthens an existing miRNA-189 target site(6), and a A1166C SNP in the angiotensin receptor 1 (AGTR1) gene abrogates its miRNA-155-mediated regulation, elevating hypertension and cardiovascular disease(7). Nevertheless, whether these phenotypes reflect mis-regulation of other targets was scarcely addressed. An exception is the pseudogene PTENP1 whose homology to the 3'UTR region of the cognate PTEN gene enables it to interact with and de-repress targets of the authentic PTEN-targeting miRNAs(8). This suggests that both coding and non-coding RNA targets that share miRNA response elements can compete for miRNA binding(9), as was demonstrated in plant starvation for miR-399(10); but thoroughly tested examples for such competition in humans are still lacking.

In both the nervous and the immune system, AChE is targeted by miR-132, which controls inflammation(4). This regulation is disturbed in numerous syndromes, including Alzheimer's disease(11), inflammatory bowel disease(12), and acute stress(13); suggesting that inherited and/or acquired interference with AChE-targeted miRs may change the outcome of diverse anxiety and inflammation-related diseases. Recently, we identified the primate-specific miR-608 as a potential AChE-targeting miRNA(14). MiR-608 is encoded by an intron of the SEMA4G gene, a member of the immunoglobulin family(15) the promoter of which includes inflammation and stress-related motifs (Supplementary Fig 1A). We hypothesized that the miR-608 multi-target effects would be particularly important for parasympathetic and anxiety-controlling genes participating in brain-to-body communication(4, 13, 16, 17)(Fig 1A). Therefore, we used this case to test the impact of the AChE 3'-UTR rs17228616 SNP(18) (www.ncbi.nlm.nih.gov/projects/SNP) located at the AChE binding site with the primate-specific miR-608 on its interactions with the validated CDC42(19) and IL6(20) targets *in vitro* and *in vivo* and the consequences of changes in these interactions.

## Results

### The primate specific miR-608 is a *bona-fide* miRNA that targets the major rs17228616 AChE allele

The 3'-UTR C2098A substitution (rs17228616) is located in the "seed"-interacting region of a putative AChE binding site to miR-608 (14, 18), close to the binding site of the AChE-targeting miR-132(4) (Figure 1B,C). However, miR-608 is unusually long (25 nucleotides), and reports of its miRNA activity were limited to heterologous systems. Therefore, we used quantitative RT-PCR to interrogate the *in vivo* expression of miR-608. These tests revealed high, medium and insignificant expression of miR-608, validated by sequencing in human intestine, brain and white blood cells (Figure 1D and Supplementary Fig 1B). Furthermore, miR-608 was efficiently co-precipitated with AGO2, identifying it as a genuine *bona fide* miRNA which functions via the AGO2 complex in spite of its being 25 nucleotides long (Figure 1E). To test the predicted miR-608/AChE interaction we cloned the AChE 3'UTR into a MicroRNA Target Selection vector carrying an upstream cytotoxic

sensor and firefly luciferase, stably-transfected human embryonic kidney 293T(HEK-293T) cells and infected these cells with miRNA-expressing lentiviruses. Cells expressing either miR-608 or miR-132 survived and showed 55% and 45% reduction in luciferase activity, respectively (n=6, one-way ANOVA: p=0.01, p=0.008, Figure 1F), reflecting functional miRNA/target interactions, whereas cells infected with a negative control lentivirus died (Supplementary Figure 1C-D). Also, human-originated U937 cells infected with miR-608 or miR-132 lentiviruses secreted less endogenous AChE compared to controls (by 21.4% and 15.1%, respectively, n=5, one-way ANOVA: p= 0.007, p=0.003) (Figure 1G), together validating AChE and cholinergic signaling as a miR-608 target. Moreover, 293T cells carrying comparable copy numbers of the major or the minor rs17228616 allele while not expressing endogenous AChE(21) (Supplementary Fig 1E) showed reduced luciferase activity under co-transfection with miR-608 by the major, but not the minor AChE 3'UTR allele (by 44%, n= 5, one-way ANOVA: p<0.001) (Figure 1H and Supplementary Fig 1F,G), indicating that the minor allele of rs17228616 reduces miR-608/AChE interaction.

**Quantifying miR-608 interaction with its targets**

Predictably, miR-608 shows thousands of potential targets (miRNAwalk: http://www.umm.uni-heidelberg.de/apps/zmf/miRNAwalk). Of those, the validated miR-608 targets Rho GTPase CDC42(19) and interleukin-6 (IL6)(20) are predictably involved in anxiety and parasympathetic signaling. Bioinformatics analysis (RNAhybrid, http://bibiserv.techfak.uni-bielefeld.de/rnahybrid/) predicted relatively tight binding to miR-608 for the C-allele and the A-allele sequences (-31.4 and -25.8 Kcal/mol), CDC42 (-26.4 Kcal/mol) and miR-132/AChE interaction (-17.3 Kcal/mol) (Figure 2A, B). To experimentally measure miR-608/target association, we adapted an *in vitro* SPR assay(22) for hybridization tests. Given that miRNA-target interactions may involve longer regions than the seed itself(1), we immobilized biotin-linked 30-mer RNA sequences of the corresponding regions in the major C-allele of AChE or CDC42 to SPR chips and injected a 25-mer RNA oligonucleotide with the miR-608 sequence. This demonstrated a ~15-fold reduction in the affinity of miR-608 to the minor A-allele compared to the C-allele AChE sequences ($K_D$ of 50.9 vs 3.1 nM, Figure 2C,D and Supplementary Fig 1H), indicating weakened A-allele AChE/miR-608 interaction. CDC42/miR-608 and AChE/miR-132 presented intermediate affinities (15.8 and 18.8 nM, Figure 2E,F), predicting a hierarchical binding preference of miR-608 to the C-allele AChE, CDC42 and the A-allele AChE target sites (Figure 2G,H).

**The minor rs17228616 allele weakens AChE suppression while potentiating suppression of other miR-608 targets**

The impaired interaction of the A-allele AChE with miR-608 predicted both weakened AChE suppression and more miR-608 molecules free to suppress other targets with tighter binding parameters, such as CDC42 and IL6 (Figure 3A). Indeed, miR-608 transfected HEK293T cells carrying the minor A-allele AChE 3'UTR showed intensified CDC42 suppression compared to those carrying the major C-allele (n= 6, one-way ANOVA: P<0.05, Figure 3B). Furthermore, miR-608 dose-dependence experiments showed increasing reductions in both AChE and CDC42 mRNA, while demonstrating that the A-allele AChE is less susceptible to miR-608 suppression and that its presence leads to enhanced suppression of CDC42 compared

to the C-allele 3'UTR, under conditions of unchanged miR-608 levels (n=5, Student's t-test: $p<0.05$ per dosage, Figure 3C).

The A-allele is relatively abundant, particularly in African-originated populations (Frequency in African ancestry (YRI, HapMap population) = 0.323; in Europeans (CEU) = 0.04). In the human brain, both CDC42 and IL6 are involved in the anxiolytic GABAergic neurotransmission and inflammatory reactions, respectively(23-25). Given the neuroimmune activities of AChE-targeting miRNAs(4, 5, 13, 14) we compared the effects of rs17228616 on CDC42 and IL6 levels in adult entorhinal cortices from The Netherlands Brain Bank(26). DNA sequencing identified three matched pairs of apparently healthy homozygotes for the minor and major rs17228616 alleles (Figure 3D and Supplementary Table 2), with indistinguishable miR-608 levels (Figure 3E). However, brain samples homozygous for the minor allele (AA) presented 65% more hydrolytic activity of AChE (Student's t-test: $p<0.05$) than homozygote major allele tissues (CC). The homologous enzyme butyrylcholinesterase (BChE)(27) showed no differences in these six samples (Figure 3F-G), demonstrating specificity. Moreover, immunoblots showed lower levels of IL6 and CDC42 in tissues homozygous for the minor compared to the major allele (Student's t-test: $p<0.05$ for both, Figure 3H-J), indicating that A-allele-related weakening of AChE suppression can increase the suppression of other miR-608 targets in the adult human brain.

CDC42, IL6 and AChE, are all causally involved with anxiety(23, 24, 28, 29). Specifically, AChE up-regulation in anxiety(30, 31) could suppress ACh levels, intercepting ACh blockade of inflammation(28), whereas the miR-608 target CDC42 interacts with collybistin in GABAergic neurons and is actively involved in formation of the anxiolytic $GABA_A$ receptor synapse (23, 32). Therefore, we predicted that rs17228616 causes additive cholinergic and GABAergic pathways-mediated increases in anxiety and parasympathetic signaling. This should impair the sympathetic control of blood pressure(33) and modify parasympathetic and anxiety phenotypes(23, 31, 34-36) in minor allele heterozygotes and homozygotes.

**Human volunteers with the minor rs17228616 allele show elevated blood pressure and reduced cortisol.**

The HERITAGE Family Study cohort (HEalth, RIsk factors, exercise Training And GEnetics) recruited young, healthy adults, of Caucasian or African-American ethnic origins(34) (see Supplementary Tables 3-4 for population characteristics). Genotyping indicated that this cohort includes 63/159 and 13/209 homozygotes or heterozygotes for the minor A-allele in the African-American and Caucasian groups, respectively (Figure 4A). Separate association analysis for the African-American and Caucasian datasets was then combined using meta-analysis. Volunteers homozygous and heterozygous for the minor A-allele showed sharply reduced serum cortisol levels and higher, albeit non-pathological systolic and diastolic blood pressure compared to homozygotes of the major C-allele ($p=9.77\times10^{-8}$; $p=0.05$; $p=0.0031$, Figure 4 B-D and Supplementary Fig 2), in spite of their young age and generally good health(34). Reduced circulating cortisol and elevated blood pressure are known factors predicting increased risks of both anxiety and hypertension-related diseases(37, 38). Also, a genome-wide association study (GWAS) in African-Americans reported significant association with hypertension for another SNP, rs78011900, in full linkage disequilibrium with rs17228616(39).

**Inhibiting brain CDC42 causes anxiety in mice**

MiR-608 is a primate-specific miRNA that does not exist in mice, but its CDC42 target(19) is expressed in the mouse brain. To test if the CDC42 suppression caused by the rs17228616 minor allele is anxiogenic, we intracerebroventricularly (ICV) injected C57Bl/6J mice with increasing doses of the CDC42 inhibitor ML141(40), until reaching a sufficient dose causing 40% decrease in its GTPase activity and mimicking the outcome in minor allele carriers (Figure 5A-B, n=5, Student's t-test:$p=0.0002$). 24 hours later, ML141-injected mice spent less time than saline-injected controls in the anxiogenic center of an open field, preferring its periphery (Fig 5C,D, n=7, Student's t-test:$p<0.01$ in all cases). Treated mice traveled similar distances, excluding motor impairments or loss of general drive (Fig 5E,F) but avoided open arms and preferred closed arms in an elevated plus maze (Fig 5G,H Student's t-test:$p<0.001$, $p<0.01$), suggesting anxiogenic reaction to CDC42 suppression.

**Discussion**

We selected the primate-specific miR-608/AChE interaction, which is naturally impaired in heterozygotes and homozygotes for the minor AChE rs17228616 allele as a case study for assessing the hierarchic potency of this specific interaction over cholinergic/parasympathetic signaling and anxiety. We established the role of miR-608 as a functioning suppressor of AChE by qPCR sequencing, SPR, luciferase and AChE activity and cell survival assays. In cultured cells and human cortices expressing the minor rs17228616 allele, we showed potentiated miR-608 suppression of CDC42 and IL6, and in experimental mice we demonstrated that excessive suppression of CDC42 indeed caused acute anxiety, supporting the notion that this could be an underlying pathway. Finally, young, healthy volunteers with the minor rs17228616 allele show elevated blood pressure and reduced cortisol, predicting risk of aging-related diseases. Taken together, these findings suggest that singly impaired miR-608/AChE interaction exacerbates the suppression of CDC42 and IL6, increasing inherited risks of anxiety and hypertension (Figure 5I).

Our study draws attention to yet elusive links between hypertension and anxiety and between those and other diseases. Elevated blood pressure often results in generalized vascular disease(41), stroke(42) and dementia(43), and thus it is a major risk factor for death. Moreover, the individual tendency to exhibit abnormally enhanced responses to stressors predicts the development of later hypertension(44). Despite the plenitude of available antihypertensive drugs, recent reports demonstrate unsatisfactory response to current treatment modalities(44) and call for disease prevention based on multiple risk factor approach(45, 46). Recently, it has been suggested that abnormal structure, function and connectivity within a cortico-limbic neural circuit in the brain leads to ‘exaggerated’ cardiovascular responses to stressors. Thus, the brain may be essential to the initiation and maintenance of blood pressure(47). However, the exact relation between the neural network and cardiovascular reactivity to stress is yet to be explored. Other as-yet non-validated targets of miR-608, and downstream changes in more miRNAs and their targets could also contribute to the complex phenotype of elevated anxiety and impaired parasympathetic function, indicating that these SNPs and the corresponding miRNA/target changes also involve elevated risk of aging-related diseases (e.g. Alzheimer’s disease(2, 48)).

We conclude that the complexity of miRNA-target interactions can affect inherited, acquired, and therapeutic interference with miRNAs, contributing to human diversities and modifying phenotypes due to cumulative effects on multiple targets. Realizing the inherited risk of delayed diseases may highlight the importance of genome information to human health and wellbeing and promote changes in life style and preventive treatment.

## Materials and methods

*AChE SNP localization:* AChE SNPs were described in Hasin et al.(18) and the NCBI dbSNP database (www.ncbi.nlm.nih.gov/snp), and co-localized with predicted miRNA binding sites to AChE according to Hanin and Soreq 2011(14).

*Lentivirus preparation:* 1 µg miRNA overexpression vectors containing pre-miR-132, -608, or a scrambled sequence (GeneCopoeia, MD, USA) 1 µg of packaging, 0.7 µg of envelope plasmid, were added to serum-free Dulbecco's Modified Eagle Medium (DMEM) supplemented with 1 mM glutamine and 50 mg/ml gentamycin. HEK-293T cells were transduced using 1mg/ml polyethylenimine (PEI) (Sigma, Israel). Virus-containing medium was collected, and stored at -80°C.

*Cell lines:* Cells were grown in a humidified atmosphere at 37°C, 5% $CO_2$. U937 cells were grown in RPMI-1640 (Sigma-Aldrich) and HEK-293T cells were grown in DMEM. Media was supplemented with 10% FBS, 2 mM L-glutamine, 1,000 units/ml penicillin, 0.1mg/ml streptomycin sulfate, and 0.25 microgram/ml amphotericin B (Beit-Haemek, Israel).

*Cholinesterase activity*: levels of catalytic activity in human brain samples and U937 cells (assayed 96 hours post-lentiviral infection) were measured using the Ellman assay as described previously.(49).

*Luciferase and life-death assay:* AChE 3'UTR sequence was cloned into the MicroRNA Target Selection System plasmid (System Biosciences, CA, USA), a dual luciferase reporter system. HEK-293T cells transfected with miRNA Target Selection-AChE 3'UTR were selected for 3 weeks. Stable cells were infected with miR-132, -608, or control sequence lentiviruses, and supplemented with cytotoxic drug 72 hours post-infection. Cell survival was determined 8 days post-infection. Luciferase activities were measured using the Dual-Luciferase® Reporter Assay (Promega, WI, USA).

*Site-directed mutagenesis:* The C2098A SNP AChE 3'UTR sequence (in pUC57) was constructed by mutagenesis, using the Quickchange II protocol (Stratagene, CA, USA) (Supplementary Figure 1G) . Major or minor allele fragments were then cloned into the psiCHECK2 vector (Promega)..

*Human samples:* Blood samples and intestinal biopsies from healthy tissue samples were obtained from volunteer participants in this study, the study was approved by the ethics committee at the Tel-Aviv Sourasky Medical Center. Postmortem cortical samples of apparently healthy aged volunteers were obtained from The Netherlands Brain Bank (NBB, Netherlands Institute for Neuroscience, Amsterdam). All material

was collected from donors whom a written informed consent for brain autopsy and the use of the material and clinical information for research purposes had been obtained by the NBB.

*AGO2-immunoprecipitation:* AGO2-immunoprecipitation was performed according to Peritz et al.(50). AGO2 was precipitated using primary antibody (sc-32877, Santa Cruz, TX, USA, 1:200), followed by qRT-PCR using qScript microRNA quantification system (Quanta Biosciences, MD, USA).

*MicroRNA-Target predicted structure and binding energy:* miRNA-target binding energy and structure were predicted using the RNAhybrid algorithm (http://bibiserv.techfak.uni-bielefeld.de/rnahybrid/).

*Surface plasmon resonance (SPR):* SPR experiments were conducted using a Biacore 3000 instrument (Biacore AB, Uppsala, Sweden). Oligonucleotides were synthesized as fully 2'O-methylated RNA. Oligos representing target mRNAs were 5' biotinylated for immobilization to the steptavidin chips (Syntezza-IDT, Israel). All sequences appear in figure 2. Standard buffer HBS (10 mM HEPES, 150 mM NaCl, 3.4 mM EDTA, 0.005% surfactant P20, pH 7.4) was used for the analyses, carried out at 25°C. Biotinylated oligonucleotides were dissolved in 100% 1,1,1,3,3,3-hexafluoro-2-propanol to 1 mM, diluted (1:5000) into 10 mM sodium acetate pH 5.0, and injected at 10 µL/min. The levels of C-allele AChE and A-allele AChE, CDC42, and AChE-miR-132 binding site captured on the chip were 325, 305, 296, and 113 RU, respectively. MiR-608 or -132 oligos were diluted in buffer (serial two-fold dilutions, 0.3125, 0.625, 1.25, 2.5, 5, and 10 µM) and injected over the flow cells for 2 min at 10 µL/min, with 5-min association & 5-min dissociation, except for the highest concentration that was allowed to dissociate for 1 hr. The sensorgrams were double-referenced and were fit using a mathematical model of a simple 1:1 interaction (Scrubber 2 software). All experiments were run in duplicate

*Immunoblots: S*amples were lysed using a 0.01 M Tris HCl pH=7.4, 1 M NaCl, 1 mM EGTA, and 1 % TX-100. SDS-PAGE separation and transfer to nitrocellulose followed standard procedures. Proteins were visualized using primary antibodies against CDC42 (ab64533, Abcam, MA, USA, 1:1000), IL6 (ab6672, Abcam, 1:1000), and GAPDH for normalization (2118, Cell Signaling, MA, USA, 1:2000), followed by horseradish peroxidase-conjugated goat anti rabbit antibodies (Jackson Laboratories, PA, USA, 1:10,000) and enhanced chemiluminescence (EZ-ECl, Biological Industries, Beit-Haemek, Israel).

*mRNA and miRNA quantification:* RNA was extracted using TRI reagent (Sigma) according to the manufacturer's protocol, followed by RNA concentration measurement (Nanodrop, Thermo, Wilmington, DE) and gel electrophoresis. cDNA synthesis (Promega, Madison, WI) was performed and mRNA levels were determined by quantitative real-time reverse transcriptase (ABI prism 7900HT, SYBR green master mix, Applied Biosystems, CA, USA). Primer sequences are listed in Supporting Information Table S1.MicroRNA levels were determined using TaqMan MicroRNA Assay (Applied Biosystems, CA, USA), or microRNA quantification system (Quanta Biosciences, MD, USA).

*Human brain tissue genotyping:* DNA was extracted using Direct PCR reagent (Viagen Biotech, CA, USA) supplemented with 0.3mg/ml proteinase K (Roche, USA). Genotyping of the A-allele of rs17228616 (C2098A) versus the C-allele was performed using TaqMan genotyping primers and AccuStart genotyping ToughMix low ROX (Quanta BioSciences, MD, USA). To differentiate further between homozygous (AA) and heterozygous (CA) rs17228616, sequencing of PCR-amplified DNA was performed.

*HERITAGE Family Study cohort*

The Health, Risk Factors, Exercise Training, and Genetics (HERITAGE) Family Study contained a total of 461 individuals (198 men and 263 women) from 150 two-generation families of African-American (172) or Caucasian (289) origin with complete data were available for this study.

*Serum Analyses:* Blood samples were collected in the morning after a 12-hour fast and serum was separated by centrifugation at 2,000 *g* (15 min at 4°C). Serum aliquots were stored at -80°C until use.

*HERITAGE sample genotyping:* Genomic DNA from previously screened individuals (34) was prepared from lymphoblastoid cell lines generated from HERITAGE samples. DNA genotyping was performed by the SNaPshot™ method (Applied Biosystems) and by sequencing.

*Statistics: P* values for the difference between the genotypes of the subjects were calculated using the likelihood ratio test. The *P* value was the exact conditional tail probability given the marginal, as was assessed by 100,000 Monte Carlo simulations. Multiple regression analysis was performed using R statistical software. Other analysis was done using R software, including meta-analysis of both populations of the cohort: African-Americans and Caucasians. Meta-analysis was performed using the "Meta" package, with fixed effects and continuous outcome data. Inverse variance weighting was used for pooling. The DerSimonian-Laird estimate for the between-study variance was used in the random effects model by default. Statistical significance was calculated using Student's *t*-test or by one- or two-way ANOVA with LSD post-hoc, where appropriate. ± SEM is shown for all graphs.

*Stereotactic injections:* All experiments were approved by the ethics committee (IACUC) of The Hebrew University (approval #12-13528-4). Seven-eight-week-old male C57Bl/6J mice were group housed until they underwent stereotaxic surgery, after which they were singly housed, at a constant temperature (22 ± 1°C) and 12-h light/dark cycles. Mice were anaesthetized by i.p. injections of ketamine (50 mg/kg; Forth Dodge, IA, USA) and domitor (0.5 mg/kg; Orion Pharma, Espoo, Finland) mix, and then mounted in a stereotaxic apparatus for intracerebroventricular injections(51). 10μM ML141 (Tocris Bioscience, Bristol, United-Kingdom ) was injected intracerebroventricularly at the following coordinates (in mm) relative to bregma: AP: −0.46, ML: ±1, DV: −2.2mm. Bilateral injections of 1 μl were conducted using a 10 μl Glenco syringe (Huston, TX, USA). After each injection, the needle was left for 5 min before being slowly retracted to allow complete diffusion.

*Behavioral analysis:*

*Elevated plus maze:* Anxiety-related behaviors were tested in a Plexiglas plus-shaped maze containing two dark and enclosed arms (30 × 5 cm with a 5 × 5 cm center area and 40 cm high walls) and two 30 × 5 cm open and lit arms, all elevated 50 cm above ground. Individual mice were placed in the center of the maze, tracked for 5 min with a video camera, and then returned to their home cage. The plus maze was wiped clean between trials with a 70% alcohol solution. Analysis was performed using EthoVision software and the Noldus system (Wageningen, The Netherlands).

*Open field:* Open Field tests were performed in a square grey plastic arena (50 x 50 cm, 40 cm high). Mice were placed in the periphery of the arena, and their behavior was recorded for 5 min using a camera. Between trials, the surface of the arena was cleaned with 70% ethanol. Behavior was analyzed using EthoVision software and the Noldus system.

*G-LISA*:
Levels of Cdc42-GTP were measured in mice hippocampi 24 hours post-injection of the CDC42 inhibitor ML141(40) using a G-LISA kit (BK127, Cytoskeleton, CO, USA) according to manufacturer's instructions. Positive controls included CDC42-GTP provided in the kit and negative controls included buffer-only samples. Repeated calibration experiments led to dose selection yielding 40% suppression of hippocampal CDC42-GTPase activity, mimicking the status of SNP minor allele humans.

**Funding**
This study was supported by the European research council (Advanced Award 321501, to H.S.).

**Acknowledgements**
The authors thank Drs David R. Bennett (Rush University's Medical Center, Chicago IL) and Michael T. Heneka (University of Bonn, Germany) for thoughtful comments, and those volunteers who donated tissues and personal details to the HERITAGE cohort and the Netherlands Brain Bank. Support of this study by the European Research Council (Advanced Award 321501, to H.S.) is acknowledged. The HERITAGE Family Study was supported by grants from the National Institutes of Health (HL45670, HL47323, HL47317, HL47327 and HL47321). Thanks are expressed to Drs Arthur S. Leon (University of Minneapolis, Minnesota), James S. Skinner (Indiana University, Indianapolis, Indiana) and Jack H. Wilmore (University of Texas at Austin, Austin, Texas) who were involved in the planning and data collection of HERITAGE. The contribution of Dr Daniel M. Landers (Arizona State University, Tempe, Arizona) to the anxiety measurements is gratefully acknowledged.

**Conflict of interest**
The authors declare no conflict of interest.

**Figure legends:**

**Figure 1: miR-608 targets the major rs17228616 AChE allele.**

(A) AChE-miRNA interactions predictably modify ACh signaling, anxiety and blood pressure. (B) Synaptic AChE mRNA (AChE-S), with the C2098A SNP in its 3' untranslated region. (C) Complementary AChE alleles, miR-608 and miR-132 sequences. Seed regions are colored and the SNP marked in yellow. (D) Endogenous expression of miR-608 in human brain and intestine tissues. (E) miR-608 expression in RNA extracted from AGO2-immunoprecipitation of extracts from HEK-293T cells stably expressing AChE 3'UTR and transfected with miR-608, control plasmid (cont) or non-treated (NT). (F) Luciferase activity of HEK-293T cells stably expressing luciferase-AChE 3'UTR and infected with miR-132, miR-608 or control lentiviruses. (G) AChE activity in human U937 lentivirus-infected U937 cells. (H) Luciferase activity of HEK-293T cells stably expressing luciferase-linked major or minor rs17228616 AChE 3'UTR alleles and infected with either miR-608 or control lentiviruses.

**Figure 2: Quantified miR-608/target interactions.**

(A) Target and miRNA RNA oligonucleotides sequences. Seed regions are colored. (B) Predicted structures and binding energy of miR-608 with AChE's C-allele and A-allele and CDC42, and of miR-132 with AChE. (C-E) SPR sensograms showing binding of miR-608 to the C-allele and A-allele of AChE and CDC42 targets. Biotinylated target RNA oligonucleotides were immobilized to a streptavidin chip and increasing concentrations (0.3125, 0.625, 1.25, 2.5, 5, 10 μM) of miRNA oligonucleotides were injected over the chip. (F) SPR sensorgrams showing miR-

132/AChE binding. (G) SPR dissociation slopes of the indicated interactions. (H) $k_a$ and $k_d$ values for the SPR reactions.

**Figure 3: The minor rs17228616 allele leads to limited suppression of AChE while potentiating CDC42 and IL6 suppression.**

(A) Experimental Hypothesis: weakened miR-608/AChE C2098A interaction would modify CDC42 and IL6 suppression. (B) A representative immunoblot and quantification of CDC42 and GAPDH in HEK-293T cells stably expressing the two AChE alleles, transfected with miR-608 or control plasmids. N=3 experiments, each in duplicates or triplicate. (C) RNA levels of AChE, CDC42, and miR-608, as a function of miR-608 plasmid dosage, (range: 0 to 1.25ug, in triplicates or duplicates); n=3 experiments. (D) Genotyped sequences of the two AChE alleles in human brain tissues. (E) Similar brain miR-608 levels in homozygous samples of both AChE alleles. (F-G) Elevated AChE but not BChE activity, in brain tissues from minor allele homozygotes. (H-J) Reduced CDC42 and IL6 in brains tissues homozygous for the minor allele.

**Figure 4: Healthy heterozygotes and homozygotes for the minor rs17228616 allele show reduced cortisol, and elevated blood pressure.**

(A) Numbers of homozygotes for the major allele and homozygotes and heterozygotes for the minor rs17228616 allele in the HERITAGE cohort. (B-D) Meta-analysis of different ethnic origins reveals reduced serum cortisol and elevated systolic and diastolic blood pressure in heterozygotes and homozygotes for the minor allele.

**Figure 5: Brain CDC42 inhibition increases anxiety in mice.**

(A) ICV injection of the CDC42 inhibitor ML141 was followed by mouse anxiety and motor functioning tests. (B) ML141 suppresses hippocampal CDC42 GTPase activity. (C-F) ML141-injected mice prefer the periphery over the center in an open field while traveling similar distances. (G-H) ML141-injected mice prefer closed over open elevated plus maze arms. (I) The major AChE allele enables balanced AChE, CDC42 and IL6 levels, which together contribute to controlling anxiety and blood pressure. The minor AChE allele enhances AChE levels and reduces CDC42 and IL6, thereby dually elevating anxiety and blood pressure.

**Supplementary Figure 1:**
(A) miR-608 is transcribed from intron 3 in the SEMA4G gene, with its promoter-binding transcription factors. (B) Representative miR-608 sequencing product from human intestine and brain. (C-D) Life and death assay of HEK-293T cells carrying AChE 3'UTR fused to cytotoxic sensor. In case of binding to the 3'UTR the cells survive but in lack of binding cells die. (E) Copy number of AChE 3'UTR in stable HEK-293T lines. (F) miR-608 expression in transfected 293T cells with prevalent or SNP AChE 3'UTR. (G) Primers used for site directed mutagenesis to create the minor allele of SNP C2098A AChE 3'UTR sequence. (H) Duplicate SPR experiment of miR-608 binding to major or minor allele of SNP C2098A in AChE.

**Supplementary Figure 2:**
**Healthy heterozygotes and homozygotes of the minor allele of C2098A SNP show elevated cortisol, and blood pressure.**
(A) Numbers of homozygotes for the major allele anf homozygotes and heterozygotes for the minor allele of SNP C2098A in the HERITAGE cohort. (B-C) Elevated serum C-reactive protein and trait, but not state anxiety in in heterozygous and homozygous of the minor allele. (D-E) Distinct distribution patterns of C-reactive protein, trait but not state anxiety, serum cortisol levels and systolic and diastolic blood pressure in heterozygous and homozygous of the minor allele. (F-G) CRP and STAT scores of heterozygous and homozygous to the minor allele compared with homozygous of the major allele.

## References


1 Bartel, D.P. (2009) MicroRNAs: target recognition and regulatory functions. *Cell*, **136**, 215-233.

2 Lau, P. and de Strooper, B. (2010) Dysregulated microRNAs in neurodegenerative disorders. *Semin Cell Dev Biol*, **21**, 768-773.

3 Filipowicz, W., Bhattacharyya, S.N. and Sonenberg, N. (2008) Mechanisms of post-transcriptional regulation by microRNAs: are the answers in sight? *Nature reviews. Genetics*, **9**, 102-114.

4 Shaked, I., Meerson, A., Wolf, Y., Avni, R., Greenberg, D., Gilboa-Geffen, A. and Soreq, H. (2009) MicroRNA-132 potentiates cholinergic anti-inflammatory signaling by targeting acetylcholinesterase. *Immunity*, **31**, 965-973.

5 Soreq, H. and Wolf, Y. (2011) NeurimmiRs: microRNAs in the neuroimmune interface. *Trends Mol Med*, **17**, 548-555.

6 Abelson, J.F., Kwan, K.Y., O'Roak, B.J., Baek, D.Y., Stillman, A.A., Morgan, T.M., Mathews, C.A., Pauls, D.L., Rasin, M.R., Gunel, M. *et al.* (2005) Sequence variants in SLITRK1 are associated with Tourette's syndrome. *Science*, **310**, 317-320.

7 Martin, M.M., Buckenberger, J.A., Jiang, J., Malana, G.E., Nuovo, G.J., Chotani, M., Feldman, D.S., Schmittgen, T.D. and Elton, T.S. (2007) The human angiotensin II type 1 receptor +1166 A/C polymorphism attenuates microrna-155 binding. *J Biol Chem*, **282**, 24262-24269.

8 Poliseno, L., Salmena, L., Zhang, J., Carver, B., Haveman, W.J. and Pandolfi, P.P. (2010) A coding-independent function of gene and pseudogene mRNAs regulates tumour biology. *Nature*, **465**, 1033-1038.

9 Salmena, L., Poliseno, L., Tay, Y., Kats, L. and Pandolfi, P.P. (2011) A ceRNA hypothesis: the Rosetta Stone of a hidden RNA language? *Cell*, **146**, 353-358.

10 Franco-Zorrilla, J.M., Valli, A., Todesco, M., Mateos, I., Puga, M.I., Rubio-Somoza, I., Leyva, A., Weigel, D., Garcia, J.A. and Paz-Ares, J. (2007) Target mimicry provides a new mechanism for regulation of microRNA activity. *Nat Genet*, **39**, 1033-1037.

11 Lau, P., Bossers, K., Salta, E., Sala Frigerio, C., Janky, R., Barbash, S., Rothman, R., Sierksma, A., Thathiah, A., Greenberg, D.S., Papadopoulou, A.S., Achsel, T., Ayoubi, T., Aerts, S., Soreq, H., Verhaagen, J., Swaab, D.F. and De Strooper, B. (2013) Alteration of the microRNA network during the progression of Alzheimer's disease. *Embo Mol Med.*, **in press**.

12 Maharshak, N., Shenhar-Tsarfaty, S., Aroyo, N., Orpaz, N., Guberman, I., Canaani, J., Halpern, Z., Dotan, I., Berliner, S. and Soreq, H. (2013) MicroRNA-132 modulates cholinergic signaling and inflammation in human inflammatory bowel disease. *Inflamm Bowel Dis*, **19**, 1346-1353.

13 Shaltiel, G., Hanan, M., Wolf, Y., Barbash, S., Kovalev, E., Shoham, S. and Soreq, H. (2013) Hippocampal microRNA-132 mediates stress-inducible cognitive deficits through its acetylcholinesterase target. *Brain Struct Funct*, **218**, 59-72.

14 Hanin, G. and Soreq, H. (2011) Cholinesterase-Targeting microRNAs Identified in silico Affect Specific Biological Processes. *Frontiers in molecular neuroscience*, **4**, 28.

15 Ryan, B.M., McClary, A.C., Valeri, N., Robinson, D., Paone, A., Bowman, E.D., Robles, A.I., Croce, C. and Harris, C.C. (2012) rs4919510 in hsa-mir-608 is associated with outcome but not risk of colorectal cancer. *PLoS ONE*, **7**, e36306.

16 Haramati, S., Navon, I., Issler, O., Ezra-Nevo, G., Gil, S., Zwang, R., Hornstein, E. and Chen, A. (2011) MicroRNA as repressors of stress-induced anxiety: the case of amygdalar miR-34. *J Neurosci*, **31**, 14191-14203.
17 Mineur, Y.S., Obayemi, A., Wigestrand, M.B., Fote, G.M., Calarco, C.A., Li, A.M. and Picciotto, M.R. (2013) Cholinergic signaling in the hippocampus regulates social stress resilience and anxiety- and depression-like behavior. *Proc Natl Acad Sci U S A*, **110**, 3573-3578.
18 Hasin, Y., Avidan, N., Bercovich, D., Korczyn, A., Silman, I., Beckmann, J.S. and Sussman, J.L. (2004) A paradigm for single nucleotide polymorphism analysis: the case of the acetylcholinesterase gene. *Hum Mutat*, **24**, 408-416.
19 Jeyapalan, Z., Deng, Z., Shatseva, T., Fang, L., He, C. and Yang, B.B. (2011) Expression of CD44 3'-untranslated region regulates endogenous microRNA functions in tumorigenesis and angiogenesis. *Nucleic Acids Res*, **39**, 3026-3041.
20 Kang, J.G., Majerciak, V., Uldrick, T.S., Wang, X., Kruhlak, M., Yarchoan, R. and Zheng, Z.M. (2011) Kaposi's sarcoma-associated herpesviral IL-6 and human IL-6 open reading frames contain miRNA binding sites and are subject to cellular miRNA regulation. *J Pathol*, **225**, 378-389.
21 Velan, B., Kronman, C., Grosfeld, H., Leitner, M., Gozes, Y., Flashner, Y., Sery, T., Cohen, S., Ben-Aziz, R., Seidman, S. *et al.* (1991) Recombinant human acetylcholinesterase is secreted from transiently transfected 293 cells as a soluble globular enzyme. *Cellular and molecular neurobiology*, **11**, 143-156.
22 Homola, J. (2008) Surface plasmon resonance sensors for detection of chemical and biological species. *Chem Rev*, **108**, 462-493.
23 Papadopoulos, T., Korte, M., Eulenburg, V., Kubota, H., Retiounskaia, M., Harvey, R.J., Harvey, K., O'Sullivan, G.A., Laube, B., Hulsmann, S. *et al.* (2007) Impaired GABAergic transmission and altered hippocampal synaptic plasticity in collybistin-deficient mice. *EMBO J*, **26**, 3888-3899.
24 Vallieres, L., Campbell, I.L., Gage, F.H. and Sawchenko, P.E. (2002) Reduced hippocampal neurogenesis in adult transgenic mice with chronic astrocytic production of interleukin-6. *J Neurosci*, **22**, 486-492.
25 Raison, C.L. and Miller, A.H. (2012) The evolutionary significance of depression in Pathogen Host Defense (PATHOS-D). *Mol Psychiatry*, in press.
26 Berson, A., Barbash, S., Shaltiel, G., Goll, Y., Hanin, G., Greenberg, D.S., Ketzef, M., Becker, A.J., Friedman, A. and Soreq, H. (2012) Cholinergic-associated loss of hnRNP-A/B in Alzheimer's disease impairs cortical splicing and cognitive function in mice. *EMBO molecular medicine*, **4**, 730-742.
27 Podoly, E., Shalev, D.E., Shenhar-Tsarfaty, S., Bennett, E.R., Ben Assayag, E., Wilgus, H., Livnah, O. and Soreq, H. (2009) The butyrylcholinesterase K variant confers structurally derived risks for Alzheimer pathology. *J Biol Chem*, **284**, 17170-17179.
28 Pavlov, V.A., Parrish, W.R., Rosas-Ballina, M., Ochani, M., Puerta, M., Ochani, K., Chavan, S., Al-Abed, Y. and Tracey, K.J. (2009) Brain acetylcholinesterase activity controls systemic cytokine levels through the cholinergic anti-inflammatory pathway. *Brain Behav Immun*, **23**, 41-45.
29 Rosas-Ballina, M., Olofsson, P.S., Ochani, M., Valdes-Ferrer, S.I., Levine, Y.A., Reardon, C., Tusche, M.W., Pavlov, V.A., Andersson, U., Chavan, S. *et al.* (2011) Acetylcholine-synthesizing T cells relay neural signals in a vagus nerve circuit. *Science*, **334**, 98-101.

30 O'Donovan, A., Hughes, B.M., Slavich, G.M., Lynch, L., Cronin, M.T., O'Farrelly, C. and Malone, K.M. (2010) Clinical anxiety, cortisol and interleukin-6: evidence for specificity in emotion-biology relationships. *Brain Behav Immun*, **24**, 1074-1077.

31 Kaufer, D., Friedman, A., Seidman, S. and Soreq, H. (1998) Acute stress facilitates long-lasting changes in cholinergic gene expression. *Nature*, **393**, 373-377.

32 Tyagarajan, S.K., Ghosh, H., Harvey, K. and Fritschy, J.M. (2011) Collybistin splice variants differentially interact with gephyrin and Cdc42 to regulate gephyrin clustering at GABAergic synapses. *J Cell Sci*, **124**, 2786-2796.

33 Guyenet, P.G. (2006) The sympathetic control of blood pressure. *Nat Rev Neurosci*, **7**, 335-346.

34 Sklan, E.H., Lowenthal, A., Korner, M., Ritov, Y., Landers, D.M., Rankinen, T., Bouchard, C., Leon, A.S., Rice, T., Rao, D.C. *et al.* (2004) Acetylcholinesterase/paraoxonase genotype and expression predict anxiety scores in Health, Risk Factors, Exercise Training, and Genetics study. *Proc Natl Acad Sci U S A*, **101**, 5512-5517.

35 Gershon, E.S., Badner, J.A., Goldin, L.R., Sanders, A.R., Cravchik, A. and Detera-Wadleigh, S.D. (1998) Closing in on genes for manic-depressive illness and schizophrenia. *Neuropsychopharmacology*, **18**, 233-242.

36 Miwa, J.M., Freedman, R. and Lester, H.A. (2011) Neural systems governed by nicotinic acetylcholine receptors: emerging hypotheses. *Neuron*, **70**, 20-33.

37 Yehuda, R. and Seckl, J. (2011) Minireview: Stress-related psychiatric disorders with low cortisol levels: a metabolic hypothesis. *Endocrinology*, **152**, 4496-4503.

38 Ong, K.L., Cheung, B.M., Man, Y.B., Lau, C.P. and Lam, K.S. (2007) Prevalence, awareness, treatment, and control of hypertension among United States adults 1999-2004. *Hypertension*, **49**, 69-75.

39 Lettre, G., Palmer, C.D., Young, T., Ejebe, K.G., Allayee, H., Benjamin, E.J., Bennett, F., Bowden, D.W., Chakravarti, A., Dreisbach, A. *et al.* (2011) Genome-wide association study of coronary heart disease and its risk factors in 8,090 African Americans: the NHLBI CARe Project. *PLoS Genet*, **7**, e1001300.

40 Martin-Granados, C., Prescott, A.R., Van Dessel, N., Van Eynde, A., Arocena, M., Klaska, I.P., Gornemann, J., Beullens, M., Bollen, M., Forrester, J.V. *et al.* (2012) A role for PP1/NIPP1 in steering migration of human cancer cells. *PLoS ONE*, **7**, e40769.

41 Akiguchi, I. and Yamamoto, Y. (2010) Vascular mechanisms of cognitive impairment: roles of hypertension and subsequent small vessel disease under sympathetic influences. *Hypertens Res*, **33**, 29-31.

42 McEwen, B.S. and Gianaros, P.J. (2011) Stress- and allostasis-induced brain plasticity. *Annu Rev Med*, **62**, 431-445.

43 Deter, H.C., Micus, C., Wagner, M., Sharma, A.M. and Buchholz, K. (2006) Salt sensitivity, anxiety, and irritability predict blood pressure increase over five years in healthy males. *Clin Exp Hypertens*, **28**, 17-27.

44 Schneider, G.M., Jacobs, D.W., Gevirtz, R.N. and O'Connor, D.T. (2003) Cardiovascular haemodynamic response to repeated mental stress in normotensive subjects at genetic risk of hypertension: evidence of enhanced reactivity, blunted adaptation, and delayed recovery. *J Hum Hypertens*, **17**, 829-840.

45 Gianaros, P.J., Onyewuenyi, I.C., Sheu, L.K., Christie, I.C. and Critchley, H.D. (2012) Brain systems for baroreflex suppression during stress in humans. *Hum Brain Mapp*, **33**, 1700-1716.
46 Gianaros, P.J., Sheu, L.K., Remo, A.M., Christie, I.C., Crtichley, H.D. and Wang, J. (2009) Heightened resting neural activity predicts exaggerated stressor-evoked blood pressure reactivity. *Hypertension*, **53**, 819-825.
47 Jennings, J.R. and Zanstra, Y. (2009) Is the brain the essential in hypertension? *Neuroimage*, **47**, 914-921.
48 Stranahan, A.M. and Mattson, M.P. (2012) Recruiting adaptive cellular stress responses for successful brain ageing. *Nat Rev Neurosci*, **13**, 209-216.
49 Ofek, K., Krabbe, K.S., Evron, T., Debecco, M., Nielsen, A.R., Brunnsgaad, H., Yirmiya, R., Soreq, H. and Pedersen, B.K. (2007) Cholinergic status modulations in human volunteers under acute inflammation. *J Mol Med (Berl)*, **85**, 1239-1251.
50 Peritz, T., Zeng, F., Kannanayakal, T.J., Kilk, K., Eiriksdottir, E., Langel, U. and Eberwine, J. (2006) Immunoprecipitation of mRNA-protein complexes. *Nat Protoc*, **1**, 577-580.
51 Barbash, S., Hanin, G. and Soreq, H. (2013) Stereotactic injection of microRNA-expressing lentiviruses to the mouse hippocampus ca1 region and assessment of the behavioral outcome. *J Vis Exp*, in press., e50170.

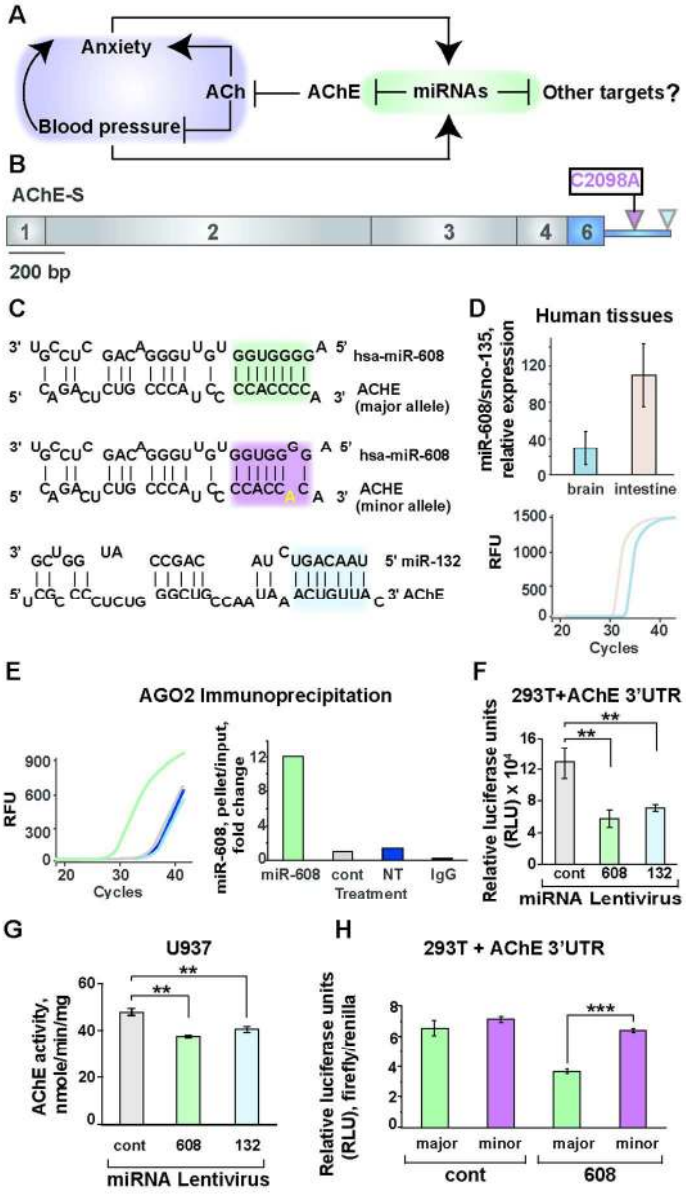


miR-608 targets the major rs17228616 AChE allele.

(A) AChE-miRNA interactions predictably modify ACh signaling, anxiety and blood pressure. (B) Synaptic AChE mRNA (AChE-S), with the C2098A SNP in its 3' untranslated region. (C) Complementary AChE alleles, miR-608 and miR-132 sequences. Seed regions are colored and the SNP marked in yellow. (D) Endogenous expression of miR-608 in human brain and intestine tissues. (E) miR-608 expression in RNA extracted from AGO2-immunoprecipitation of extracts from HEK-293T cells stably expressing AChE 3'UTR and transfected with miR-608, control plasmid (cont) or non-treated (NT). (F) Luciferase activity of HEK-293T cells stably expressing luciferase-AChE 3'UTR and infected with miR-132, miR-608 or control lentiviruses. (G) AChE activity in human U937 lentivirus-infected U937 cells. (H) Luciferase activity of HEK-293T cells stably expressing luciferase-linked major or minor rs17228616 AChE 3'UTR alleles and infected with either miR-608 or control lentiviruses.

89x152mm (300 x 300 DPI)

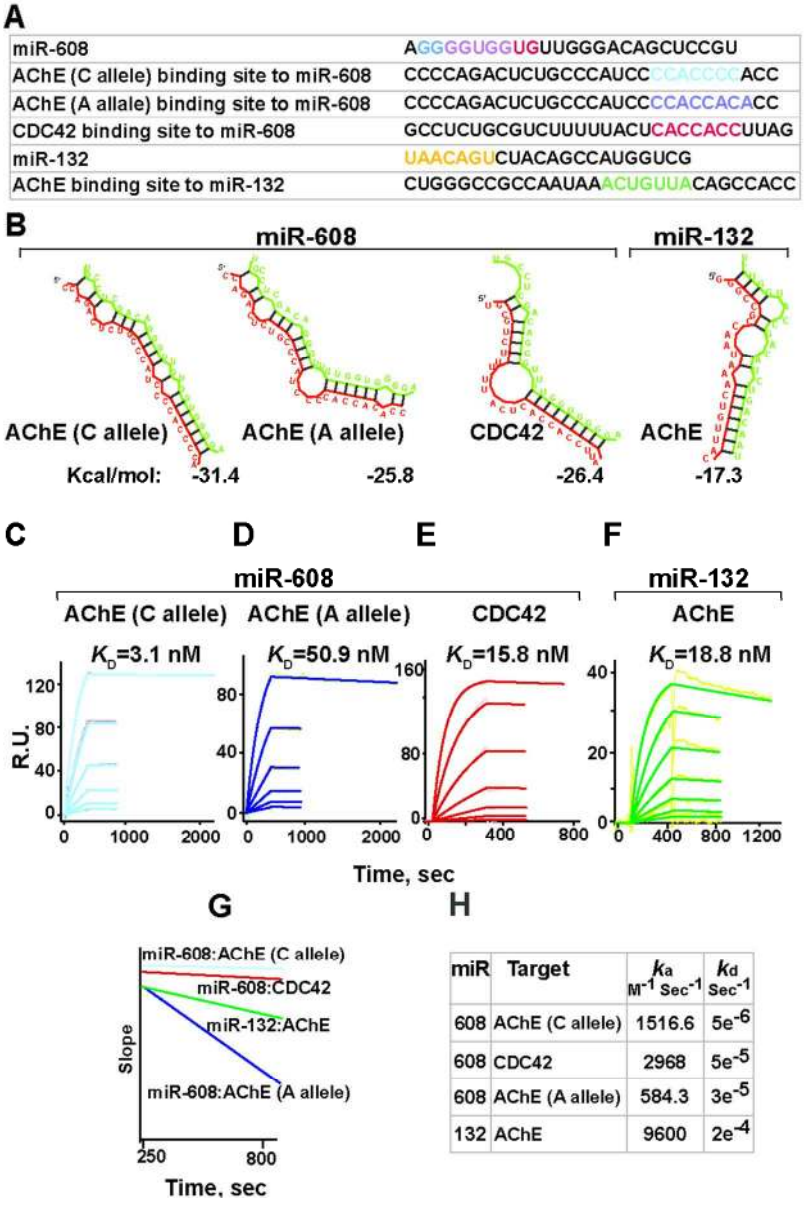


| miR | Target | $k_a$ $M^{-1}$ $Sec^{-1}$ | $k_d$ $Sec^{-1}$ |
|---|---|---|---|
| 608 | AChE (C allele) | 1516.6 | $5e^{-6}$ |
| 608 | CDC42 | 2968 | $5e^{-5}$ |
| 608 | AChE (A allele) | 584.3 | $3e^{-5}$ |
| 132 | AChE | 9600 | $2e^{-4}$ |

Quantified miR-608/target interactions.
(A) Target and miRNA RNA oligonucleotides sequences. Seed regions are colored. (B) Predicted structures and binding energy of miR-608 with AChE's C-allele and A-allele and CDC42, and of miR-132 with AChE. (C-E) SPR sensograms showing binding of miR-608 to the C-allele and A-allele of AChE and CDC42 targets. Biotinylated target RNA oligonucleotides were immobilized to a streptavidin chip and increasing concentrations (0.3125, 0.625, 1.25, 2.5, 5, 10 μM) of miRNA oligonucleotides were injected over the chip. (F) SPR sensorgrams showing miR-132/AChE binding. (G) SPR dissociation slopes of the indicated interactions. (H) ka and kd values for the SPR reactions.
89x130mm (300 x 300 DPI)

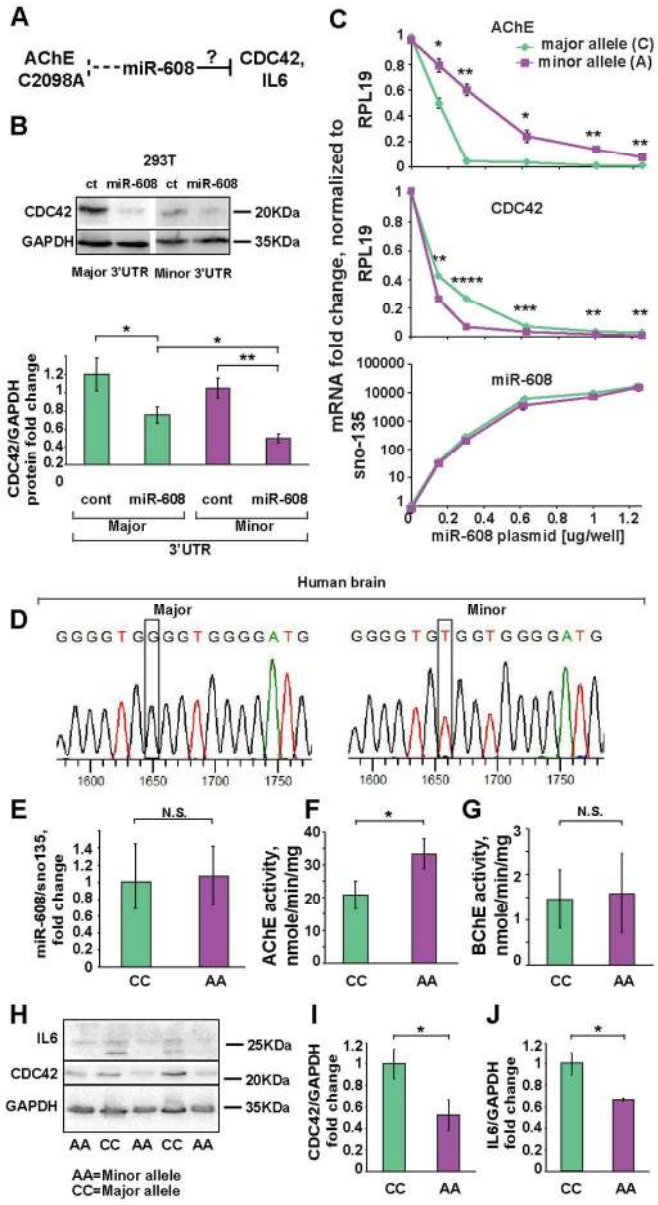


The minor rs17228616 allele leads to limited suppression of AChE while potentiating CDC42 and IL6 suppression.

(A) Experimental Hypothesis: weakened miR-608/AChE C2098A interaction would modify CDC42 and IL6 suppression. (B) A representative immunoblot and quantification of CDC42 and GAPDH in HEK-293T cells stably expressing the two AChE alleles, transfected with miR-608 or control plasmids. N=3 experiments, each in duplicates or triplicate. (C) RNA levels of AChE, CDC42, and miR-608, as a function of miR-608 plasmid dosage, (range: 0 to 1.25ug, in triplicates or duplicates); n=3 experiments. (D) Genotyped sequences of the two AChE alleles in human brain tissues. (E) Similar brain miR-608 levels in homozygous samples of both AChE alleles. (F-G) Elevated AChE but not BChE activity, in brain tissues from minor allele homozygotes. (H-J) Reduced CDC42 and IL6 in brains tissues homozygous for the minor allele.

89x161mm (300 x 300 DPI)

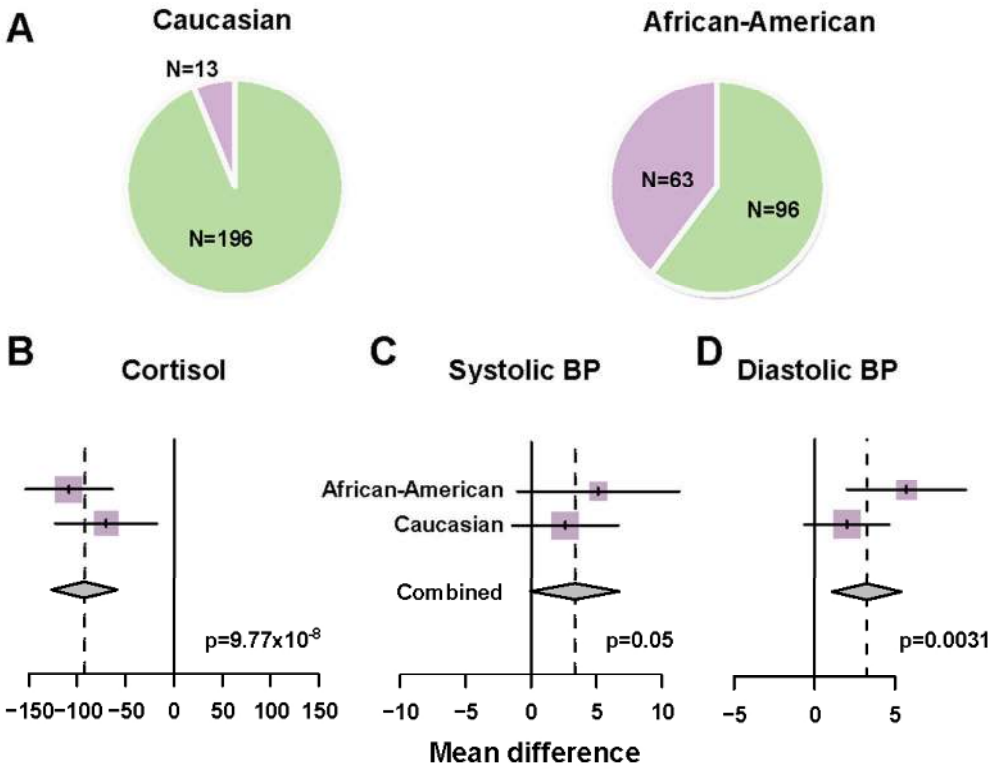


Healthy heterozygotes and homozygotes for the minor rs17228616 allele show reduced cortisol, and elevated blood pressure.
(A) Numbers of homozygotes for the major allele and homozygotes and heterozygotes for the minor rs17228616 allele in the HERITAGE cohort. (B-D) Meta-analysis of different ethnic origins reveals reduced serum cortisol and elevated systolic and diastolic blood pressure in heterozygotes and homozygotes for the minor allele.

89x69mm (300 x 300 DPI)

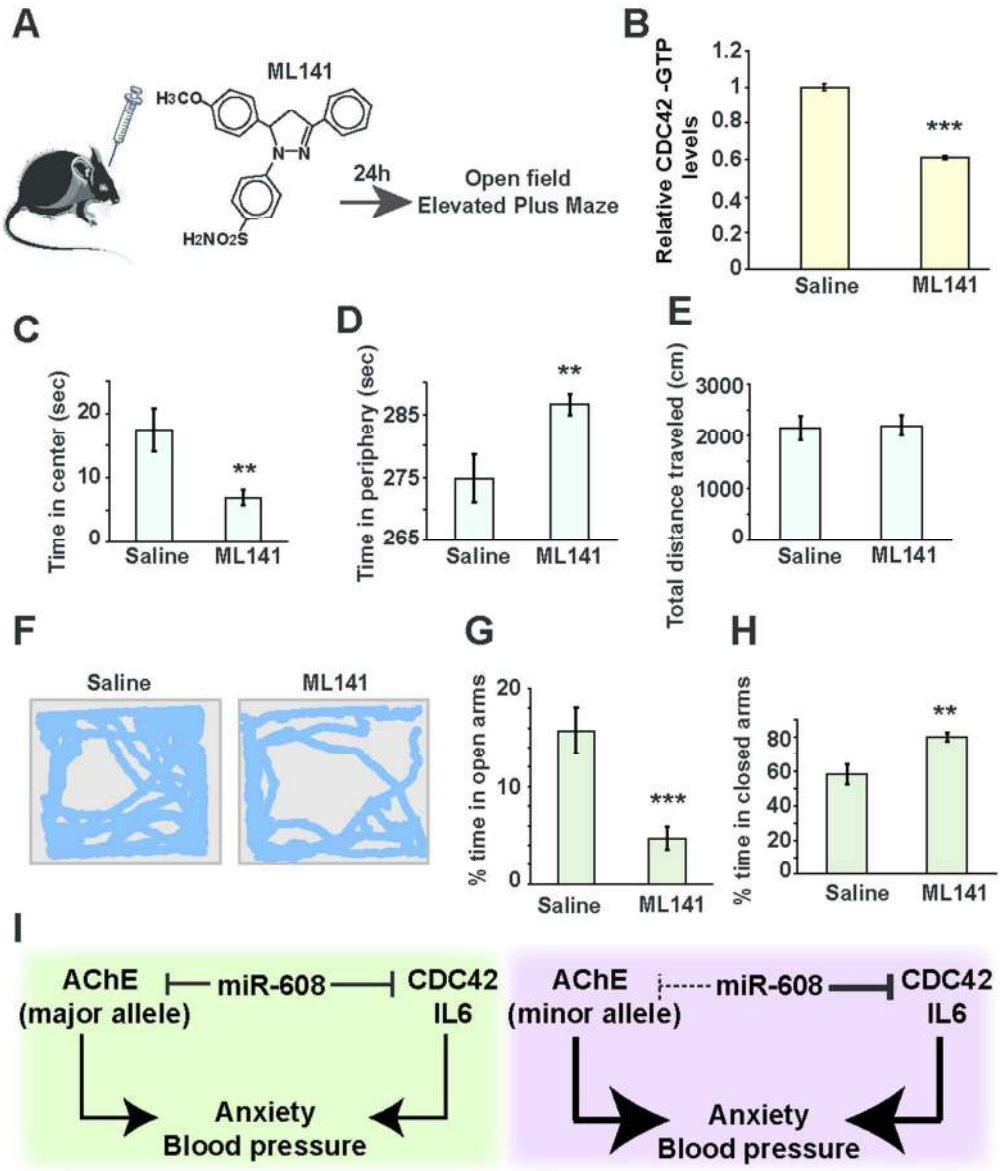


Brain CDC42 inhibition increases anxiety in mice.
(A) ICV injection of the CDC42 inhibitor ML141 was followed by mouse anxiety and motor functioning tests. (B) ML141 suppresses hippocampal CDC42 GTPase activity. (C-F) ML141-injected mice prefer the periphery over the center in an open field while traveling similar distances. (G-H) ML141-injected mice prefer closed over open elevated plus maze arms. (I) The major AChE allele enables balanced AChE, CDC42 and IL6 levels, which together contribute to controlling anxiety and blood pressure. The minor AChE allele enhances AChE levels and reduces CDC42 and IL6, thereby dually elevating anxiety and blood pressure.

89x104mm (300 x 300 DPI)

04.03.14

Dear Prof. Davies,

Thank you for the constructive review of our manuscript.

We found the reviewers' comments both informative and important, performed much additional work and revised our manuscript accordingly. A new figure has been added, and the text was revised as well. We thank the reviewers for addressing the weakness points in this study and made an effort to strengthen these points as recommended. In addition, we prepared a suggested cover image for this article which has also been submitted. Please see below our detailed point-by-point answers to the reviewers' comments.

All formatting errors found in the manuscript were corrected according to the instructions.

We are particularly grateful to reviewer no. 2 for his/her in-depth review, and for the satisfaction with our experimental design and technical performance.

Reviewer no. 1 commented:

"In HEK293T cells there is a 3-fold repression of the luciferase reporter by miR-608 (Fig 1F), whereas a minor effect is observed at the level of AChE activity in U937 cells. What happens at the AChE protein levels in U937 cells? "

We found this comment important and performed an immunoblot analysis for the AChE protein in U937 cells exposed to miR-608 compared to controls. A robust effect was observed at the level of the AChE protein, and, as we previously showed, this effect was considerably larger than that observed in the catalytic activity of the AChE enzyme, compatible with a large fraction of the AChE protein being catalytically inactive (as we previously reported in Shaked et al. Immunity 2009). Fig 1G in the manuscript had been revised accordingly, demonstrating a similarly robust suppression of the AChE protein by miR-132 and miR-608.

"The authors argue that the reduced interaction between miR-608 and AChE in the presence of the minor allele potentiates the repression of other miR-608 targets. However the Western-blot shown in Fig. 3B does not corroborate this conclusion/claim. "

To refine the presentation we replaced the presented blot with a more representative one. We hope that the outcome of greater difference between the control and the miR-608 treated cells for the major and minor alleles will be clearer in this revised figure.

"Moreover, for the in vitro experiments the authors restrict their analysis to CDC42 (Fig 3B and C), while arguing for the same effect in other targets (e.g. IL-6). It is essential to check the effect for additional miR-608 targets. Along this line, it would be most interesting to use a genome-wide approach to look at the overall targets of miR-608."

We found this comment of utmost importance for understanding the complexity aspect of miR-608 effects. To address this issue more globally, we used the miRwalk database (http://www.umm.uni-heidelberg.de/apps/zmf/mirwalk/) to identify the top

30 predicted targets of miR-608, searched for those targets that are expressed in HEK293T cells (which incidentally do not express IL6) and designed RT-PCR primers for all of these predicted targets(Supplementary Table 2). We then performed a microfluidics dynamic array experiment (Fluidigm http://www.fluidigm.com/biomark-hd-system.html) to simultaneously quantify the levels of all of those predicted targets in cells carrying the major and minor alleles of the AChE 3'-UTR and treated with increasing doses of miR-608. Among those, we identified 3 genes (NACC1, mapped to Chr 19p13.2, with 7 putative binding sites for miR-608; TPP1, mapped to Chr 11p15, with 2 binding sites; and the validated target CD44, mapped to Chr 11p13, with one binding site) that showed similar behavior to that of CDC42 mapped to Ch 1p36.1 and IL6 mapped to Chr 7p15.3, suppression of both of which we show in human post-mortem cortices). Briefly, all of these transcripts showed dose-dependent suppression by miR-608 and cells carrying the minor A-allele presented potentiated suppression of these targets compared to those carrying the major C-allele. Thus, we have now showed that the studied SNP in the AChE gene caused allele-specific difference between the capacity of miR-608 to suppress its other targets; that this effect is not limited to CDC42 and IL6, that it does not depend on the number of miR-608 binding sites in those other targets and that it is evident in at least 4 different chromosomes. These new observations were now added to the text under Results; the quantification is presented in the revised Figure 3 (as Figure 3D), and the remaining part of Fig3 became the new Fig4, with the other figures re-numbered successively. We also added the Fluidigm procedure to the revised Methods and referred to the implications of these measurements under Discussion.

"In the experiments shown in Fig 3B and 3C, AChE 3'UTR reporter constructs containing the major allele and minor allele were introduced in HEK293T cells. How do the levels of these reporter constructs compare with the levels of AChE in cell types expressing AChE? It would be more informative to perform these experiments in a cellular model that expresses AChE and use the same background to construct minor allele mutant. "

We accept this comment; however, AChE expression levels are rather low in most cell types excluding mature differentiated brain neurons and erythrocytes, to an extent that would jeopardize measurements of expression in cells carrying the different alleles. Given this difficulty, we selected HEK293T cells that do not express endogenous AChE, which reduces the background signal to extremely low levels, and transfected them with parallel levels of the major and minor allele 3'-UTR constructs. To check the effect in those cell types expressing the native AChE alleles we interrogated post-mortem tissue samples removed from the human brain, where we could genotype the AChE alleles, determine AChE activity in the native tissue and quantify CDC42 and IL6 levels.

" The Western-blots shown in Fig 3H for CDC42 and IL6 should be improved, so that reliable quantifications can be obtained (Fig 3I and IJ). In addition it would be important to show the protein levels of AChE in these samples. "

The presentation of the IL6 western blot has been improved, and is now presented in the new Figure 4E. The protein levels of AChE were tested in HEK293T cells (revised Figure 1).

"Color legend is missing for Fig 4."

We added the color legend to the figure.

We would like to thank reviewer no. 1 again for these important comments, and believe that the introduced changes (highlighted in yellow throughout the text) improved the quality of our article.

Sincerely,

Hermona Soreq, PhD

Professor of Molecular Neuroscience

The Edmond and Lily Safra center for Brain Sciences

The Hebrew University of Jerusalem

The Edmond J. Safra Campus, Givat Ram

Jerusalem 91904 ISRAEL

Tel No: 972-2-6585109

Fax No: 972-2-6520258

Email: hermona.soreq@mail.huji.ac.il

# Competing targets of microRNA-608 affect anxiety and hypertension

Geula Hanin[1], Shani Shenhar-Tsarfaty[1], Nadav Yayon[1], Yau Yin Hoe[2], Estelle R. Bennett[1], Ella H. Sklan[3], Dabeeru. C. Rao[4], Tuomo Rankinen[5], Claude Bouchard[5], Susana Geifman-Shochat[2], Sagiv Shifman[1], David S. Greenberg[1], and Hermona Soreq[1*]

[1] The Silberman Institute of Life Sciences, The Hebrew University of Jerusalem, Givat Ram, Jerusalem 91904, Israel, and The Edmond and Lily Safra Center for Brain Science.

[2] School of Biological Sciences, Nanyang Technological University, 60 Nanyang Avenue, Singapore 637551

[3] Department of Clinical Microbiology and Immunology, Sackler School of Medicine, Tel Aviv University, Tel Aviv 69978, Israel,

[4] Division of Biostatistics, School of Medicine, Washington University in St. Louis, St. Louis, MO, USA.

[5] Human Genomics Laboratory, Pennington Biomedical Research Center, Baton Rouge, LA, USA

*To whom correspondence should be addressed: Prof. Hermona Soreq, The Edmond and Lily Safra Center for Brain Sciences, The Hebrew University of Jerusalem, The Edmond Safra Campus, Givat Ram, Jerusalem 91904, Israel. Tel: 972-2-658-5109; Fax: 972-2-652-0258 E-mail: hermona.soreq@mail.huji.ac.il.



## Abstract

MicroRNAs (miRNAs) can repress multiple targets, but how a single de-balanced interaction affects others remained unclear. We found that changing a single miRNA-target interaction can simultaneously affect multiple other miRNA-target interactions, and modify physiological phenotype. We show that miR-608 targets acetylcholinesterase (AChE) and demonstrate weakened miR-608 interaction with the rs17228616 AChE allele having a single nucleotide polymorphism (SNP) in the 3'-

untranslated region (3'UTR). In cultured cells, this weakened interaction potentiated miR-608-mediated suppression of other targets, including CDC42 and interleukin-6 (IL6). Post-mortem human cortices homozygote for the minor rs17228616 allele showed AChE elevation and CDC42/IL6 decreases compared to major allele homozygotes. Additionally, minor allele heterozygote and homozygote subjects showed reduced cortisol and elevated blood pressure, predicting risk of anxiety and hypertension. Parallel suppression of the conserved brain CDC42 activity by intracerebroventricular ML141 injection caused acute anxiety in mice. We demonstrate that single SNPs in miRNA-binding regions could cause expanded downstream effects changing important biological pathways.



## Introduction

MiRNAs are short non-coding RNAs, 20-25 nucleotides long, that can simultaneously regulate multiple genes in biological pathways(1) by post-transcriptionally suppressing translation and/or inducing degradation of their mRNA targets(1-3), suggesting that they are particularly suitable for controlling the rapidly adjustable physiology of the parasympathetic system. Moreover, due to the multileveled activities of Acetylcholine (ACh) signaling, miRNAs could modulate both the neuronal and immune functions of ACh by controlling its production and elimination(4, 5). However, the biological impact of maintaining multiple miRNA-target interactions balanced, the inherited diversity of miRNA regulation or how impairments in one interaction would affect the others has not been thoroughly addressed(5).

SNP interference with miRNA functions affects the expression of corresponding

targets, modifies brain functions and induces a risk of disease. In Tourette's syndrome, a 3'-UTR SNP in the brain-expressed human Slit and Trk-like-1 (SLITRK1) gene strengthens an existing miRNA-189 target site(6), and a A1166C SNP in the angiotensin receptor 1 (AGTR1) gene abrogates its miRNA-155-mediated regulation, exacerbating the risk of hypertension and cardiovascular disease(7). Nevertheless, whether these phenotypes reflect mis-regulation of other targets was scarcely addressed. An exception is the pseudogene PTENP1 whose homology to the 3'UTR region of the cognate PTEN gene enables it to interact with and de-repress targets of the authentic PTEN-targeting miRNAs(8). This suggests that both coding and non-coding RNA targets that share miRNA response elements can compete for miRNA binding(9, 10), as was demonstrated in plant starvation for miR-399(11); but thoroughly tested examples for such competition in humans are still lacking.

In both the nervous and the immune system, the ACh hydrolyzing enzyme acetylcholinesterase (AChE) is targeted by miR-132, which controls inflammation(4). This regulation is disturbed in numerous syndromes, including Alzheimer's disease(12), inflammatory bowel disease(13), and acute stress(14); suggesting that inherited and/or acquired interference with AChE-targeted miRs may change the outcome of diverse anxiety and inflammation-related diseases. Recently, we identified the primate-specific miR-608 (14) as a potential AChE-targeting miRNA. MiR-608 is encoded by an intron of the SEMA4G gene, a member of the immunoglobulin family(15) the promoter of which includes inflammation and stress-related motifs (Supplementary Fig 1A). We hypothesized that the miR-608 multi-target effects would be particularly important for parasympathetic and anxiety-controlling genes participating in brain-to-body communication(4, 14, 16, 17)(Fig 1A). Therefore, we

used this case to test the impact of the AChE 3'-UTR rs17228616 SNP(18) (www.ncbi.nlm.nih.gov/projects/SNP) located at the AChE binding site with the primate-specific miR-608 on its interactions with the validated CDC42(19) and IL6(20) targets *in vitro* and *in vivo* and the consequences of changes in these interactions.

## Results

### The primate specific miR-608 is a *bona-fide* miRNA that targets the major rs17228616 AChE allele

The 3'-UTR C2098A substitution (rs17228616) is located in the "seed"-interacting region of a putative AChE binding site to miR-608 (18, 21), close to the binding site of the AChE-targeting miR-132(4) (Figure 1B,C). However, miR-608 is unusually long (25 nucleotides), and reports of its miRNA activity were limited to heterologous systems. Therefore, we used quantitative RT-PCR to interrogate the *in vivo* expression of miR-608. These tests revealed high, medium and insignificant expression of miR-608, validated by sequencing in human intestine, brain and white blood cells (Figure 1D and Supplementary Fig 1B). Furthermore, miR-608 was efficiently co-precipitated with AGO2, identifying it as a genuine *bona fide* miRNA which functions via the AGO2 complex in spite of its being 25 nucleotides long (Figure 1E). To test the predicted miR-608/AChE interaction we cloned the AChE 3'UTR into a MicroRNA Target Selection vector carrying an upstream cytotoxic sensor and firefly luciferase, stably-transfected human embryonic kidney 293T(HEK-293T) cells and infected these cells with miRNA-expressing lentiviruses. Cells expressing either miR-608 or miR-132 survived and showed 55% and 45% reduction in luciferase activity, respectively (n=6, one-way ANOVA: p=0.01, p=0.008, Figure

1F), reflecting functional miRNA/target interactions, whereas cells infected with a negative control lentivirus died (Supplementary Figure 1C-D). Also, human-originated U937 cells infected with miR-608 or miR-132 lentiviruses secreted less endogenous AChE compared to controls (by 21.4% and 15.1%, respectively, n=5, one-way ANOVA: p= 0.007, p=0.003). Both catalytic AChE activities and AChE protein levels in U937 cells infected with miR-608 or miR-132 lentiviruses were substantially reduced, (n=3, one-way ANOVA: p= 0.024, p=0.026, Figure 1G), together validating AChE and the cholinergic signaling pathway as being targeted by miR-608. Moreover, transfecting the AChE non-expressing 293T cells (21) to carry comparable copy numbers of the major or the minor rs17228616 allele (Supplementary Fig 1E) showed reduced luciferase activity under co-transfection with miR-608 by the major, but not the minor AChE 3'UTR allele (by 44%, n= 5, one-way ANOVA: p<0.001) (Figure 1H and Supplementary Fig 1F,G), indicating that the minor allele of rs17228616 reduces miR-608/AChE interaction.

**Quantifying miR-608 interaction with its targets**

Predictably, miR-608 shows thousands of potential targets (miRNAwalk: http://www.umm.uni-heidelberg.de/apps/zmf/miRNAwalk). Of those, the validated miR-608 targets Rho GTPase CDC42(19) and interleukin-6 (IL6)(20) are predictably involved in anxiety and parasympathetic signaling. Bioinformatics analysis (RNAhybrid, http://bibiserv.techfak.uni-bielefeld.de/rnahybrid/) predicted relatively tight binding to miR-608 for the C-allele and the A-allele sequences (-31.4 and -25.8 Kcal/mol), CDC42 (-26.4 Kcal/mol) and miR-132/AChE interaction (-17.3 Kcal/mol) (Figure 2A, B). To experimentally measure miR-608/target association, we adapted an *in vitro* Surface Plasmon Resonance (SPR) assay(22) for hybridization tests. Given

that miRNA-target interactions may involve longer regions than the seed itself(1), we immobilized biotin-linked 30-mer RNA sequences of the corresponding regions in the major C-allele of AChE or CDC42 to SPR chips and injected a 25-mer RNA oligonucleotide with the miR-608 sequence. This demonstrated a ~15-fold reduction in the affinity of miR-608 to the minor A-allele compared to the C-allele AChE sequences ($K_D$ of 50.9 vs 3.1 nM, Figure 2C,D and Supplementary Fig 1H), indicating weakened A-allele AChE/miR-608 interaction. CDC42/miR-608 and AChE/miR-132 presented intermediate affinities (15.8 and 18.8 nM, Figure 2E,F), predicting a hierarchical binding preference of miR-608 to the C-allele AChE, CDC42 and the A-allele AChE target sites (Figure 2G,H).

**The minor rs17228616 allele weakens AChE suppression while potentiating suppression of other miR-608 targets**

The impaired interaction of the A-allele AChE with miR-608 predicted both weakened AChE suppression and more miR-608 molecules free to suppress other targets with tighter binding parameters, such as CDC42 and IL6 (Figure 3A). Indeed, miR-608 transfected HEK293T cells carrying the minor A-allele AChE 3'UTR showed intensified CDC42 suppression compared to those carrying the major C-allele (n=6, one-way ANOVA: $P<0.05$, Figure 3B). Furthermore, miR-608 dose-dependence experiments showed increasing reductions in both AChE and CDC42 mRNA, while demonstrating that the A-allele AChE is less susceptible to miR-608 suppression and that its presence leads to enhanced suppression of CDC42 compared to the C-allele 3'UTR, under conditions of unchanged miR-608 levels (n=5, Student's t-test: $p<0.05$ per dosage, Figure 3C). To test the hypothesis that parallel effects exist for additional miR-608 targets, we identified the top predicted targets of miR-608 by

multiple algorithms according to the miRwalk database (http://www.umm.uni-heidelberg.de/apps/zmf/mirwalk/) and designed a microfluidics dynamic array experiment (Fluidigm, http://www.fluidigm.com/biomark-hd-system.html) to simultaneously and comparatively quantify changes in those predicted targets that are expressed in these cells (raw data in Supplementary Table 2). Three of the tested genes showed parallel differences to those observed for CDC42 and IL6. These were NACC1, mapped to Chromosome 19p13.2, known to alter the HMGB1-mediated autophagic response (23) and carrying 7 predicted binding sites for miR-608; the Chromosome 11p15 TPP1 tripeptidyl-peptidase 1 lipid metabolism regulating enzyme (24), with two predicted sites for miR-608 and the Chromosome 11p13 validated angiogenesis regulating target CD44(19), with one binding site for miR-608. Enhanced suppression of each of these putative target genes in cells carrying the A-allele compared to the C-allele (Figure 3D) demonstrated that this effect extends beyond CDC42 and IL6 differences and that it occurs in transcripts of different chromosomal origins carrying different numbers of miR-608 binding sites.

The A-allele is relatively abundant, particularly in African-originated populations (Frequency in African ancestry (YRI, HapMap population) = 0.323; in Europeans (CEU) = 0.04). In the human brain, both CDC42 and IL6 are involved in the anxiolytic GABAergic neurotransmission and inflammatory reactions, respectively(25-27). Given the neuroimmune activities of AChE-targeting miRNAs(4, 5, 14, 21) we compared the effects of rs17228616 on CDC42 and IL6 levels in adult entorhinal cortices from The Netherlands Brain Bank(28). DNA sequencing identified three matched pairs of apparently healthy homozygotes for the minor and major rs17228616 alleles (Figure 4A and Supplementary Table 3), with indistinguishable

miR-608 levels (Figure 4B). However, brain samples homozygous for the minor allele (AA) presented 65% more hydrolytic activity of AChE (Student's t-test: $p<0.05$) than homozygote major allele tissues (CC). The homologous enzyme butyrylcholinesterase (BChE)(29) showed no differences in these six samples (Figure 4C-D), demonstrating specificity. Moreover, immunoblots showed lower levels of IL6 and CDC42 in tissues homozygous for the minor compared to the major allele (Student's t-test: $p<0.05$ for both, Figure 4E-G), indicating that A-allele-related weakening of AChE suppression can increase the suppression of other miR-608 targets in the adult human brain.

CDC42, IL6 and AChE, are all causally involved with anxiety(25, 26, 30, 31). Specifically, AChE up-regulation in anxiety(32, 33) could suppress ACh levels, intercepting ACh blockade of inflammation(30), whereas the miR-608 target CDC42 interacts with collybistin in GABAergic neurons and is actively involved in formation of the anxiolytic $GABA_A$ receptor synapse (25, 34). Therefore, we predicted that rs17228616 causes additive cholinergic and GABAergic pathways-mediated increases in anxiety and parasympathetic signaling. This should impair the sympathetic control of blood pressure(35) and modify parasympathetic and anxiety phenotypes(25, 33, 36-38) in minor allele heterozygotes and homozygotes.

**Human volunteers with the minor rs17228616 allele show elevated blood pressure and reduced cortisol.**

The HERITAGE Family Study cohort (HEalth, RIsk factors, exercise Training And GEnetics) recruited young, healthy adults, of Caucasian or African-American ethnic origins(36) (see Supplementary Tables 4-5 for population characteristics). Genotyping indicated that this cohort includes 63/159 and 13/209 homozygotes or heterozygotes

for the minor A-allele in the African-American and Caucasian groups, respectively (Figure 5A). Separate association analysis for the African-American and Caucasian datasets was then combined using meta-analysis. Volunteers homozygous and heterozygous for the minor A-allele showed sharply reduced serum cortisol levels and higher, albeit non-pathological systolic and diastolic blood pressure compared to homozygotes of the major C-allele ($p=9.77x10^{-8}$; p=0.05; p=0.0031, Figure 5B-D and Supplementary Fig 2), in spite of their young age and generally good health(36). Reduced circulating cortisol and elevated blood pressure are known factors predicting increased risks of both anxiety and hypertension-related diseases(39, 40). Also, a genome-wide association study (GWAS) in African-Americans reported significant association with hypertension for another SNP, rs78011900, in full linkage disequilibrium with rs17228616(41).

**Inhibiting brain CDC42 causes anxiety in mice**

MiR-608 is a primate-specific miRNA that does not exist in mice, but its CDC42 target(19) is expressed in the mouse brain. To test if the CDC42 suppression caused by the rs17228616 minor allele is anxiogenic, we intracerebroventricularly (ICV) injected C57Bl/6J mice with increasing doses of the CDC42 inhibitor ML141(42), until reaching a sufficient dose causing 40% decrease in its GTPase activity and mimicking the outcome in minor allele carriers (Figure 6A-B, n=5, Student's t-test:p=0.0002). 24 hours later, ML141-injected mice spent less time than saline-injected controls in the anxiogenic center of an open field, preferring its periphery (Figure 6C,D, n=7, Student's t-test:$p<0.01$ in all cases). Treated mice traveled similar distances, excluding motor impairments or loss of general drive (Figure 6E,F) but avoided open arms and preferred closed arms in an elevated plus maze (Figure 6G,H

Student's t-test:$p<0.001$, $p<0.01$), suggesting anxiogenic reaction to CDC42 suppression.

**Discussion**

We selected the primate-specific miR-608/AChE interaction, which is naturally impaired in heterozygotes and homozygotes for the minor AChE rs17228616 allele as a case study for assessing the hierarchic potency of this specific interaction over cholinergic/parasympathetic signaling and anxiety. We established the role of miR-608 as a functioning suppressor of AChE by qPCR sequencing, SPR, luciferase and AChE activity and cell survival assays. In cultured cells and human cortices expressing the minor rs17228616 allele, we showed potentiated miR-608 suppression of CDC42 and IL6. Excessive suppression of CDC42 caused acute anxiety, supporting the notion that this could be an underlying pathway; and microfluidics dynamic array tests showed enhanced suppression of the validated miR-608 target CD44 and the predicted NACC1 and TPP1 targets in cells carrying the minor (A) compared to the major (C) allele. CD44 is known for its involvement in hematopoietic tumors (19), NACC1 is involved in proliferation, apoptosis and transcriptional regulation(23), and TPP1 functions in the lysosome to cleave N-terminal tripeptides (24), suggesting potentially wider implications of rs17228616 in cancer and neurodegenerative disease. Supporting this notion, young, healthy volunteers with the minor rs17228616 allele show elevated blood pressure and reduced cortisol, predicting risk of aging-related diseases. Taken together, these findings suggest that singly impaired miR-608/AChE interaction exacerbates the suppression of CDC42, IL6, CDC44 and possibly other targets, increasing inherited risks of anxiety and hypertension (Figure 6I).

Our study draws attention to the evolutionary importance of co-regulated changes in primate-specific miRNAs and their targets for higher brain functions at large (43) as well as to miRNA regulation of cholinergic signaling (44) and the elusive links between hypertension, anxiety and other diseases. Elevated blood pressure often results in generalized vascular disease(45), stroke(46) and dementia(47), and thus it is a major risk factor for death. Moreover, the individual tendency to exhibit abnormally enhanced responses to stressors predicts the development of later hypertension(48). Despite the plentitude of available antihypertensive drugs, recent reports demonstrate unsatisfactory response to current treatment modalities(48) and call for disease prevention based on multiple risk factor approach(49, 50). Recently, it has been suggested that abnormal structure, function and connectivity within a cortico-limbic neural circuit in the brain leads to 'exaggerated' cardiovascular responses to stressors. Thus, the brain may be essential to the initiation and maintenance of blood pressure(51). However, the exact relation between the neural network and cardiovascular reactivity to stress is yet to be explored. Other as-yet non-validated targets of miR-608, and downstream changes in more miRNAs and their targets could also contribute to the complex phenotype of elevated anxiety and impaired parasympathetic function, indicating that these SNPs and the corresponding miRNA/target changes also involve elevated risk of aging-related diseases (e.g. Alzheimer's disease(2, 52)).

We conclude that the complexity of miRNA-target interactions can affect inherited, acquired, and therapeutic interference with miRNAs, contributing to human diversities and modifying phenotypes due to cumulative effects on multiple targets.

Realizing the inherited risk of delayed diseases may highlight the importance of genome information to human health and wellbeing and promote changes in life style and preventive treatment.

**Materials and Methods**

*AChE SNP localization:* AChE SNPs were described in Hasin et al.(18) and the NCBI dbSNP database (www.ncbi.nlm.nih.gov/snp), and co-localized with predicted miRNA binding sites to AChE according to Hanin and Soreq 2011(21).

*Lentivirus preparation:* 1 µg miRNA overexpression vectors containing pre-miR-132, -608, or a scrambled sequence (GeneCopoeia, MD, USA) 1 µg of packaging, 0.7 µg of envelope plasmid, were added to serum-free Dulbecco's Modified Eagle Medium (DMEM) supplemented with 1 mM glutamine and 50 mg/ml gentamycin. HEK-293T cells were transduced using 1mg/ml polyethylenimine (PEI) (Sigma, Israel). Virus-containing medium was collected, and stored at -80°C.

*Cell lines:* Cells were grown in a humidified atmosphere at 37°C, 5% $CO_2$. U937 cells were grown in RPMI-1640 (Sigma-Aldrich) and HEK-293T cells were grown in DMEM. Media was supplemented with 10% FBS, 2 mM L-glutamine, 1,000 units/ml penicillin, 0.1mg/ml streptomycin sulfate, and 0.25 microgram/ml amphotericin B (Beit-Haemek, Israel).

*Cholinesterase activity*: levels of catalytic activity in human brain samples and U937 cells (assayed 96 hours post-lentiviral infection) were measured using the Ellman assay as described previously.(53).

*Luciferase and life-death assay:* AChE 3'UTR sequence was cloned into the MicroRNA Target Selection System plasmid (System Biosciences, CA, USA), a dual luciferase reporter system. HEK-293T cells transfected with miRNA Target Selection-AChE 3'UTR were selected for 3 weeks. Stable cells were infected with miR-132, -608, or control sequence lentiviruses, and supplemented with cytotoxic drug 72 hours post-infection. Cell survival was determined 8 days post-infection. Luciferase activities were measured using the Dual-Luciferase® Reporter Assay (Promega, WI, USA).

*Site-directed mutagenesis:* The C2098A SNP AChE 3'UTR sequence (in pUC57) was constructed by mutagenesis, using the Quickchange II protocol (Stratagene, CA, USA) (Supplementary Figure 1G) . Major or minor allele fragments were then cloned into the psiCHECK2 vector (Promega)..

*Human samples:* Blood samples and intestinal biopsies from healthy tissue samples were obtained from volunteer participants in this study, the study was approved by the ethics committee at the Tel-Aviv Sourasky Medical Center. Postmortem cortical samples of apparently healthy aged volunteers were obtained from The Netherlands Brain Bank (NBB, Netherlands Institute for Neuroscience, Amsterdam). All material was collected from donors whom a written informed consent for brain autopsy and the use of the material and clinical information for research purposes had been obtained by the NBB.

*AGO2-immunoprecipitation:* AGO2-immunoprecipitation was performed according to Peritz et al.(54). AGO2 was precipitated using primary antibody (sc-32877, Santa Cruz, TX, USA, 1:200), followed by qRT-PCR using qScript microRNA quantification system (Quanta Biosciences, MD, USA).

*MicroRNA-Target predicted structure and binding energy:* miRNA-target binding energy and structure were predicted using the RNAhybrid algorithm (http://bibiserv.techfak.uni-bielefeld.de/rnahybrid/).

*Surface plasmon resonance (SPR):* SPR experiments were conducted using a Biacore 3000 instrument (Biacore AB, Uppsala, Sweden). Oligonucleotides were synthesized as fully 2'O-methylated RNA. Oligos representing target mRNAs were 5' biotinylated for immobilization to the steptavidin chips (Syntezza-IDT, Israel). All sequences appear in figure 2. Standard buffer HBS (10 mM HEPES, 150 mM NaCl, 3.4 mM EDTA, 0.005% surfactant P20, pH 7.4) was used for the analyses, carried out at 25°C. Biotinylated oligonucleotides were dissolved in 100% 1,1,1,3,3,3-hexafluoro-2-propanol to 1 mM, diluted (1:5000) into 10 mM sodium acetate pH 5.0, and injected at 10 µL/min. The levels of C-allele AChE and A-allele AChE, CDC42, and AChE-miR-132 binding site captured on the chip were 325, 305, 296, and 113 RU, respectively. MiR-608 or -132 oligos were diluted in buffer (serial two-fold dilutions, 0.3125, 0.625, 1.25, 2.5, 5, and 10 µM) and injected over the flow cells for 2 min at 10 µL/min, with 5-min association & 5-min dissociation, except for the highest concentration that was allowed to dissociate for 1 hr. The sensorgrams were double-referenced and were fit using a mathematical model of a simple 1:1 interaction (Scrubber 2 software). All experiments were run in duplicate

*Immunoblots: S*amples were lysed using a 0.01 M Tris HCl pH=7.4, 1 M NaCl, 1 mM EGTA, and 1 % TX-100. SDS-PAGE separation and transfer to nitrocellulose followed standard procedures. Proteins were visualized using primary antibodies against CDC42 (ab64533, Abcam, MA, USA, 1:1000), IL6 (ab6672, Abcam, 1:1000), AChE (sc-6431, Santa Cruz Biotechnology, 1:200) and GAPDH for normalization (2118, Cell Signaling, MA, USA, 1:2000), followed by horseradish peroxidase-conjugated goat anti rabbit antibodies (Jackson Laboratories, PA, USA, 1:10,000) and enhanced chemiluminescence (EZ-ECl, Biological Industries, Beit-Haemek, Israel).

*mRNA and miRNA quantification:* RNA was extracted using TRI reagent (Sigma) according to the manufacturer's protocol, followed by RNA concentration measurement (Nanodrop, Thermo, Wilmington, DE) and gel electrophoresis. cDNA synthesis (Promega, Madison, WI) was performed and mRNA levels were determined by quantitative real-time reverse transcriptase (ABI prism 7900HT, SYBR green master mix, Applied Biosystems, CA, USA). Primer sequences are listed in Supporting Information Table S1.MicroRNA levels were determined using TaqMan MicroRNA Assay (Applied Biosystems, CA, USA), or microRNA quantification system (Quanta Biosciences, MD, USA).

*Human brain tissue genotyping:* DNA was extracted using Direct PCR reagent (Viagen Biotech, CA, USA) supplemented with 0.3mg/ml proteinase K (Roche, USA). Genotyping of the A-allele of rs17228616 (C2098A) versus the C-allele was performed using TaqMan genotyping primers and AccuStart genotyping ToughMix low ROX (Quanta BioSciences, MD, USA). To differentiate further between

homozygous (AA) and heterozygous (CA) rs17228616, sequencing of PCR-amplified DNA was performed.

*Fluidigm*

Expression of the top predicted targets of miR-608 was determined using a high-throughput microfluidic qRT-PCR instrument (BioMark, Fluidigm, San Francisco, CA). Preamplified cDNA samples were mixed with TaqMan PreAmp Master Mix (Applied Biosystems) and DDW and pipetted into the Dynamic Fluidigm Array 48x48 chip. Amplification reaction product was cleaned using Exonuclease I (New England Biolabs, Ipswitch MA), and diluted 1:5 in Tris-EDTA buffer, pH=8. qRT-PCR mix was prepared using 2x SsoFast EvaGreen Supermix with low ROX (Biorad, Hercules CA). Priming and loading was performed using IFC Controller HX (BioMark). All qRT-PCR reactions were performed using the GE 48x48 PCR+Melt v2.pcl protocol. Data analysis involved BioMark Real-Time PCR Analysis Software Version 2.0 (Fluidigm), and the ΔCt method was applied.

*HERITAGE Family Study cohort*

The Health, Risk Factors, Exercise Training, and Genetics (HERITAGE) Family Study contained a total of 461 individuals (198 men and 263 women) from 150 two-generation families of African-American (172) or Caucasian (289) origin with complete data were available for this study.

*Serum Analyses:* Blood samples were collected in the morning after a 12-hour fast and serum was separated by centrifugation at 2,000 *g* (15 min at 4°C). Serum aliquots were stored at -80°C until use.

*HERITAGE sample genotyping:* Genomic DNA from previously screened individuals (36) was prepared from lymphoblastoid cell lines generated from HERITAGE samples. DNA genotyping was performed by the SNaPshot™ method (Applied Biosystems) and by sequencing.

*Statistics: P* values for the difference between the genotypes of the subjects were calculated using the likelihood ratio test. The *P* value was the exact conditional tail probability given the marginal, as was assessed by 100,000 Monte Carlo simulations. Multiple regression analysis was performed using R statistical software. Other analysis was done using R software, including meta-analysis of both populations of the cohort: African-Americans and Caucasians. Meta-analysis was performed using the "Meta" package, with fixed effects and continuous outcome data. Inverse variance weighting was used for pooling. The DerSimonian-Laird estimate for the between-study variance was used in the random effects model by default. Statistical significance was calculated using Student's *t*-test or by one- or two-way ANOVA with LSD post-hoc, where appropriate. ± SEM is shown for all graphs.

*Stereotactic injections:* All experiments were approved by the ethics committee (IACUC) of The Hebrew University (approval #12-13528-4). Seven-eight-week-old male C57Bl/6J mice were group housed until they underwent stereotaxic surgery, after which they were singly housed, at a constant temperature (22 ± 1°C) and 12-h light/dark cycles. Mice were anaesthetized by i.p. injections of ketamine (50 mg/kg; Forth Dodge, IA, USA) and domitor (0.5 mg/kg; Orion Pharma, Espoo, Finland) mix, and then mounted in a stereotaxic apparatus for intracerebroventricular injections(55).

10µM ML141 (Tocris Bioscience, Bristol, United-Kingdom ) was injected intracerebroventricularly at the following coordinates (in mm) relative to bregma: AP: −0.46, ML: ±1, DV: −2.2mm. Bilateral injections of 1 µl were conducted using a 10 µl Glenco syringe (Huston, TX, USA). After each injection, the needle was left for 5 min before being slowly retracted to allow complete diffusion.

*Behavioral analysis:*

*Elevated plus maze:* Anxiety-related behaviors were tested in a Plexiglas plus-shaped maze containing two dark and enclosed arms (30 × 5 cm with a 5 × 5 cm center area and 40 cm high walls) and two 30 × 5 cm open and lit arms, all elevated 50 cm above ground. Individual mice were placed in the center of the maze, tracked for 5 min with a video camera, and then returned to their home cage. The plus maze was wiped clean between trials with a 70% alcohol solution. Analysis was performed using EthoVision software and the Noldus system (Wageningen, The Netherlands).

*Open field:* Open Field tests were performed in a square grey plastic arena (50 x 50 cm, 40 cm high). Mice were placed in the periphery of the arena, and their behavior was recorded for 5 min using a camera. Between trials, the surface of the arena was cleaned with 70% ethanol. Behavior was analyzed using EthoVision software and the Noldus system.

*G-LISA*:

Levels of Cdc42-GTP were measured in mice hippocampi 24 hours post-injection of the CDC42 inhibitor ML141(42) using a G-LISA kit (BK127, Cytoskeleton, CO, USA) according to manufacturer's instructions. Positive controls included CDC42-GTP provided in the kit and negative controls included buffer-only samples. Repeated

calibration experiments led to dose selection yielding 40% suppression of hippocampal CDC42-GTPase activity, mimicking the status of SNP minor allele humans.

**Acknowledgements**

The authors thank Drs David R. Bennett (Rush University's Medical Center, Chicago IL) and Michael T. Heneka (University of Bonn, Germany) for thoughtful comments, and those volunteers who donated tissues and personal details to the HERITAGE cohort and the Netherlands Brain Bank. Support of this study by the European Research Council (Advanced Award 321501, to H.S.) is acknowledged. The HERITAGE Family Study was supported by grants from the National Institutes of Health (HL45670, HL47323, HL47317, HL47327 and HL47321). Thanks are expressed to Drs Arthur S. Leon (University of Minneapolis, Minnesota), James S. Skinner (Indiana University, Indianapolis, Indiana) and Jack H. Wilmore (University of Texas at Austin, Austin, Texas) who were involved in the planning and data collection of HERITAGE. The contribution of Dr Daniel M. Landers (Arizona State University, Tempe, Arizona) to the anxiety measurements is gratefully acknowledged.

**Conflict of interest**

The authors declare no conflict of interest.

**References**

1 Bartel, D.P. (2009) MicroRNAs: target recognition and regulatory functions. *Cell*, **136**, 215-233.

2 Lau, P. and de Strooper, B. (2010) Dysregulated microRNAs in neurodegenerative disorders. *Semin Cell Dev Biol*, **21**, 768-773.

3 Filipowicz, W., Bhattacharyya, S.N. and Sonenberg, N. (2008) Mechanisms of post-transcriptional regulation by microRNAs: are the answers in sight? *Nature reviews. Genetics*, **9**, 102-114.
4 Shaked, I., Meerson, A., Wolf, Y., Avni, R., Greenberg, D., Gilboa-Geffen, A. and Soreq, H. (2009) MicroRNA-132 potentiates cholinergic anti-inflammatory signaling by targeting acetylcholinesterase. *Immunity*, **31**, 965-973.
5 Soreq, H. and Wolf, Y. (2011) NeurimmiRs: microRNAs in the neuroimmune interface. *Trends Mol Med*, **17**, 548-555.
6 Abelson, J.F., Kwan, K.Y., O'Roak, B.J., Baek, D.Y., Stillman, A.A., Morgan, T.M., Mathews, C.A., Pauls, D.L., Rasin, M.R., Gunel, M. *et al.* (2005) Sequence variants in SLITRK1 are associated with Tourette's syndrome. *Science*, **310**, 317-320.
7 Martin, M.M., Buckenberger, J.A., Jiang, J., Malana, G.E., Nuovo, G.J., Chotani, M., Feldman, D.S., Schmittgen, T.D. and Elton, T.S. (2007) The human angiotensin II type 1 receptor +1166 A/C polymorphism attenuates microrna-155 binding. *J Biol Chem*, **282**, 24262-24269.
8 Poliseno, L., Salmena, L., Zhang, J., Carver, B., Haveman, W.J. and Pandolfi, P.P. (2010) A coding-independent function of gene and pseudogene mRNAs regulates tumour biology. *Nature*, **465**, 1033-1038.
9 Salmena, L., Poliseno, L., Tay, Y., Kats, L. and Pandolfi, P.P. (2011) A ceRNA hypothesis: the Rosetta Stone of a hidden RNA language? *Cell*, **146**, 353-358.
10 Tay, Y., Rinn, J. and Pandolfi, P.P. (2014) The multilayered complexity of ceRNA crosstalk and competition. *Nature*, **505**, 344-352.
11 Franco-Zorrilla, J.M., Valli, A., Todesco, M., Mateos, I., Puga, M.I., Rubio-Somoza, I., Leyva, A., Weigel, D., Garcia, J.A. and Paz-Ares, J. (2007) Target mimicry provides a new mechanism for regulation of microRNA activity. *Nat Genet*, **39**, 1033-1037.
12 Lau, P., Bossers, K., Salta, E., Sala Frigerio, C., Janky, R., Barbash, S., Rothman, R., Sierksma, A., Thathiah, A., Greenberg, D.S., Papadopoulou, A.S., Achsel, T., Ayoubi, T., Aerts, S., Soreq, H., Verhaagen, J., Swaab, D.F. and De Strooper, B. (2013) Alteration of the microRNA network during the progression of Alzheimer's disease. *Embo Mol Med.*, **in press**.
13 Maharshak, N., Shenhar-Tsarfaty, S., Aroyo, N., Orpaz, N., Guberman, I., Canaani, J., Halpern, Z., Dotan, I., Berliner, S. and Soreq, H. (2013) MicroRNA-132 modulates cholinergic signaling and inflammation in human inflammatory bowel disease. *Inflamm Bowel Dis*, **19**, 1346-1353.
14 Shaltiel, G., Hanan, M., Wolf, Y., Barbash, S., Kovalev, E., Shoham, S. and Soreq, H. (2013) Hippocampal microRNA-132 mediates stress-inducible cognitive deficits through its acetylcholinesterase target. *Brain Struct Funct*, **218**, 59-72.
15 Ryan, B.M., McClary, A.C., Valeri, N., Robinson, D., Paone, A., Bowman, E.D., Robles, A.I., Croce, C. and Harris, C.C. (2012) rs4919510 in hsa-mir-608 is associated with outcome but not risk of colorectal cancer. *PLoS ONE*, **7**, e36306.
16 Haramati, S., Navon, I., Issler, O., Ezra-Nevo, G., Gil, S., Zwang, R., Hornstein, E. and Chen, A. (2011) MicroRNA as repressors of stress-induced anxiety: the case of amygdalar miR-34. *J Neurosci*, **31**, 14191-14203.
17 Mineur, Y.S., Obayemi, A., Wigestrand, M.B., Fote, G.M., Calarco, C.A., Li, A.M. and Picciotto, M.R. (2013) Cholinergic signaling in the hippocampus

regulates social stress resilience and anxiety- and depression-like behavior. *Proc Natl Acad Sci U S A*, **110**, 3573-3578.

18 Hasin, Y., Avidan, N., Bercovich, D., Korczyn, A., Silman, I., Beckmann, J.S. and Sussman, J.L. (2004) A paradigm for single nucleotide polymorphism analysis: the case of the acetylcholinesterase gene. *Hum Mutat*, **24**, 408-416.

19 Jeyapalan, Z., Deng, Z., Shatseva, T., Fang, L., He, C. and Yang, B.B. (2011) Expression of CD44 3'-untranslated region regulates endogenous microRNA functions in tumorigenesis and angiogenesis. *Nucleic Acids Res*, **39**, 3026-3041.

20 Kang, J.G., Majerciak, V., Uldrick, T.S., Wang, X., Kruhlak, M., Yarchoan, R. and Zheng, Z.M. (2011) Kaposi's sarcoma-associated herpesviral IL-6 and human IL-6 open reading frames contain miRNA binding sites and are subject to cellular miRNA regulation. *J Pathol*, **225**, 378-389.

21 Hanin, G. and Soreq, H. (2011) Cholinesterase-Targeting microRNAs Identified in silico Affect Specific Biological Processes. *Frontiers in molecular neuroscience*, **4**, 28.

22 Homola, J. (2008) Surface plasmon resonance sensors for detection of chemical and biological species. *Chem Rev*, **108**, 462-493.

23 Zhang, Y., Cheng, Y., Ren, X., Zhang, L., Yap, K.L., Wu, H., Patel, R., Liu, D., Qin, Z.H., Shih, I.M. *et al.* (2012) NAC1 modulates sensitivity of ovarian cancer cells to cisplatin by altering the HMGB1-mediated autophagic response. *Oncogene*, **31**, 1055-1064.

24 Guhaniyogi, J., Sohar, I., Das, K., Stock, A.M. and Lobel, P. (2009) Crystal structure and autoactivation pathway of the precursor form of human tripeptidyl-peptidase 1, the enzyme deficient in late infantile ceroid lipofuscinosis. *The Journal of biological chemistry*, **284**, 3985-3997.

25 Papadopoulos, T., Korte, M., Eulenburg, V., Kubota, H., Retiounskaia, M., Harvey, R.J., Harvey, K., O'Sullivan, G.A., Laube, B., Hulsmann, S. *et al.* (2007) Impaired GABAergic transmission and altered hippocampal synaptic plasticity in collybistin-deficient mice. *EMBO J*, **26**, 3888-3899.

26 Vallieres, L., Campbell, I.L., Gage, F.H. and Sawchenko, P.E. (2002) Reduced hippocampal neurogenesis in adult transgenic mice with chronic astrocytic production of interleukin-6. *J Neurosci*, **22**, 486-492.

27 Raison, C.L. and Miller, A.H. (2012) The evolutionary significance of depression in Pathogen Host Defense (PATHOS-D). *Mol Psychiatry*, in press.

28 Berson, A., Barbash, S., Shaltiel, G., Goll, Y., Hanin, G., Greenberg, D.S., Ketzef, M., Becker, A.J., Friedman, A. and Soreq, H. (2012) Cholinergic-associated loss of hnRNP-A/B in Alzheimer's disease impairs cortical splicing and cognitive function in mice. *EMBO molecular medicine*, **4**, 730-742.

29 Podoly, E., Shalev, D.E., Shenhar-Tsarfaty, S., Bennett, E.R., Ben Assayag, E., Wilgus, H., Livnah, O. and Soreq, H. (2009) The butyrylcholinesterase K variant confers structurally derived risks for Alzheimer pathology. *J Biol Chem*, **284**, 17170-17179.

30 Pavlov, V.A., Parrish, W.R., Rosas-Ballina, M., Ochani, M., Puerta, M., Ochani, K., Chavan, S., Al-Abed, Y. and Tracey, K.J. (2009) Brain acetylcholinesterase activity controls systemic cytokine levels through the cholinergic anti-inflammatory pathway. *Brain Behav Immun*, **23**, 41-45.

31 Rosas-Ballina, M., Olofsson, P.S., Ochani, M., Valdes-Ferrer, S.I., Levine, Y.A., Reardon, C., Tusche, M.W., Pavlov, V.A., Andersson, U., Chavan, S. *et al.*

(2011) Acetylcholine-synthesizing T cells relay neural signals in a vagus nerve circuit. *Science*, **334**, 98-101.
32 O'Donovan, A., Hughes, B.M., Slavich, G.M., Lynch, L., Cronin, M.T., O'Farrelly, C. and Malone, K.M. (2010) Clinical anxiety, cortisol and interleukin-6: evidence for specificity in emotion-biology relationships. *Brain Behav Immun*, **24**, 1074-1077.
33 Kaufer, D., Friedman, A., Seidman, S. and Soreq, H. (1998) Acute stress facilitates long-lasting changes in cholinergic gene expression. *Nature*, **393**, 373-377.
34 Tyagarajan, S.K., Ghosh, H., Harvey, K. and Fritschy, J.M. (2011) Collybistin splice variants differentially interact with gephyrin and Cdc42 to regulate gephyrin clustering at GABAergic synapses. *J Cell Sci*, **124**, 2786-2796.
35 Guyenet, P.G. (2006) The sympathetic control of blood pressure. *Nat Rev Neurosci*, **7**, 335-346.
36 Sklan, E.H., Lowenthal, A., Korner, M., Ritov, Y., Landers, D.M., Rankinen, T., Bouchard, C., Leon, A.S., Rice, T., Rao, D.C. *et al.* (2004) Acetylcholinesterase/paraoxonase genotype and expression predict anxiety scores in Health, Risk Factors, Exercise Training, and Genetics study. *Proc Natl Acad Sci U S A*, **101**, 5512-5517.
37 Gershon, E.S., Badner, J.A., Goldin, L.R., Sanders, A.R., Cravchik, A. and Detera-Wadleigh, S.D. (1998) Closing in on genes for manic-depressive illness and schizophrenia. *Neuropsychopharmacology*, **18**, 233-242.
38 Miwa, J.M., Freedman, R. and Lester, H.A. (2011) Neural systems governed by nicotinic acetylcholine receptors: emerging hypotheses. *Neuron*, **70**, 20-33.
39 Yehuda, R. and Seckl, J. (2011) Minireview: Stress-related psychiatric disorders with low cortisol levels: a metabolic hypothesis. *Endocrinology*, **152**, 4496-4503.
40 Ong, K.L., Cheung, B.M., Man, Y.B., Lau, C.P. and Lam, K.S. (2007) Prevalence, awareness, treatment, and control of hypertension among United States adults 1999-2004. *Hypertension*, **49**, 69-75.
41 Lettre, G., Palmer, C.D., Young, T., Ejebe, K.G., Allayee, H., Benjamin, E.J., Bennett, F., Bowden, D.W., Chakravarti, A., Dreisbach, A. *et al.* (2011) Genome-wide association study of coronary heart disease and its risk factors in 8,090 African Americans: the NHLBI CARe Project. *PLoS Genet*, **7**, e1001300.
42 Martin-Granados, C., Prescott, A.R., Van Dessel, N., Van Eynde, A., Arocena, M., Klaska, I.P., Gornemann, J., Beullens, M., Bollen, M., Forrester, J.V. *et al.* (2012) A role for PP1/NIPP1 in steering migration of human cancer cells. *PLoS ONE*, **7**, e40769.
43 Barbash, S., Shifman, S. and Soreq, H. (In Press) Global co-evolution of human microRNAs and their target genes. *Molecular Biology and Evolution*, in press.
44 Nadorp, B. and Soreq, H. (2014) Predicted overlapping microRNA regulators of acetylcholine packaging and degradation in neuroinflammation-related disorders. *Frontiers in molecular neuroscience*, **7**.
45 Akiguchi, I. and Yamamoto, Y. (2010) Vascular mechanisms of cognitive impairment: roles of hypertension and subsequent small vessel disease under sympathetic influences. *Hypertens Res*, **33**, 29-31.
46 McEwen, B.S. and Gianaros, P.J. (2011) Stress- and allostasis-induced brain plasticity. *Annu Rev Med*, **62**, 431-445.

47 Deter, H.C., Micus, C., Wagner, M., Sharma, A.M. and Buchholz, K. (2006) Salt sensitivity, anxiety, and irritability predict blood pressure increase over five years in healthy males. *Clin Exp Hypertens*, **28**, 17-27.
48 Schneider, G.M., Jacobs, D.W., Gevirtz, R.N. and O'Connor, D.T. (2003) Cardiovascular haemodynamic response to repeated mental stress in normotensive subjects at genetic risk of hypertension: evidence of enhanced reactivity, blunted adaptation, and delayed recovery. *J Hum Hypertens*, **17**, 829-840.
49 Gianaros, P.J., Onyewuenyi, I.C., Sheu, L.K., Christie, I.C. and Critchley, H.D. (2012) Brain systems for baroreflex suppression during stress in humans. *Hum Brain Mapp*, **33**, 1700-1716.
50 Gianaros, P.J., Sheu, L.K., Remo, A.M., Christie, I.C., Crtichley, H.D. and Wang, J. (2009) Heightened resting neural activity predicts exaggerated stressor-evoked blood pressure reactivity. *Hypertension*, **53**, 819-825.
51 Jennings, J.R. and Zanstra, Y. (2009) Is the brain the essential in hypertension? *Neuroimage*, **47**, 914-921.
52 Stranahan, A.M. and Mattson, M.P. (2012) Recruiting adaptive cellular stress responses for successful brain ageing. *Nat Rev Neurosci*, **13**, 209-216.
53 Ofek, K., Krabbe, K.S., Evron, T., Debecco, M., Nielsen, A.R., Brunnsgaad, H., Yirmiya, R., Soreq, H. and Pedersen, B.K. (2007) Cholinergic status modulations in human volunteers under acute inflammation. *J Mol Med (Berl)*, **85**, 1239-1251.
54 Peritz, T., Zeng, F., Kannanayakal, T.J., Kilk, K., Eiriksdottir, E., Langel, U. and Eberwine, J. (2006) Immunoprecipitation of mRNA-protein complexes. *Nat Protoc*, **1**, 577-580.
55 Barbash, S., Hanin, G. and Soreq, H. (2013) Stereotactic injection of microRNA-expressing lentiviruses to the mouse hippocampus ca1 region and assessment of the behavioral outcome. *J Vis Exp*, in press., e50170.

**Figure legends:**

**Figure 1: miR-608 targets the major rs17228616 AChE allele.**

(A) AChE-miRNA interactions predictably modify ACh signaling, anxiety and blood pressure. (B) Synaptic AChE mRNA (AChE-S), with the C2098A SNP in its 3' untranslated region. (C) Complementary AChE alleles, miR-608 and miR-132 sequences. Seed regions are colored and the SNP marked in yellow. (D) Endogenous expression of miR-608 in human brain and intestine tissues. (E) miR-608 expression in RNA extracted from AGO2-immunoprecipitation of extracts from HEK-293T cells stably expressing AChE 3'UTR and transfected with miR-608, control plasmid (cont) or non-treated (NT). (F) Luciferase activity of HEK-293T cells stably expressing

luciferase-AChE 3'UTR and infected with miR-132, miR-608 or control lentiviruses. (G) AChE activity and representative immunoblot and quantification in human U937 lentivirus-infected U937 cells. (H) Luciferase activity of HEK-293T cells stably expressing luciferase-linked major or minor rs17228616 AChE 3'UTR alleles and infected with either miR-608 or control lentiviruses.

**Figure 2: Quantified miR-608/target interactions.**

(A) Target and miRNA RNA oligonucleotides sequences. Seed regions are colored. (B) Predicted structures and binding energy of miR-608 with AChE's C-allele and A-allele and CDC42, and of miR-132 with AChE. (C-E) SPR sensograms showing binding of miR-608 to the C-allele and A-allele of AChE and CDC42 targets. Biotinylated target RNA oligonucleotides were immobilized to a streptavidin chip and increasing concentrations (0.3125, 0.625, 1.25, 2.5, 5, 10 μM) of miRNA oligonucleotides were injected over the chip. (F) SPR sensorgrams showing miR-132/AChE binding. (G) SPR dissociation slopes of the indicated interactions. (H) $k_a$ and $k_d$ values for the SPR reactions.

**Figure 3: Cells carrying the minor rs17228616 allele show limited suppression of AChE and potentiated suppression of CDC42, IL6 and other predicted targets.**

(A) Experimental Hypothesis: weakened miR-608/AChE C2098A interaction would modify CDC42 and IL6 suppression. (B) A representative immunoblot and quantification of CDC42 and GAPDH in HEK-293T cells stably expressing the two AChE alleles, transfected with miR-608 or control plasmids. N=3 experiments, each in duplicates or triplicate. (C) RNA levels of AChE, CDC42, and miR-608, as a function of miR-608 plasmid dosage, (range: 0 to 1.25ug, in triplicates or duplicates);

n=3 experiments. (D) RNA levels of NACC1, TPP1 and CD44 by miR-608 obtained in a Fluidigm test of pooled samples as in C.

**Figure 4: Human brain samples carrying the minor rs17228616 allele show elevated AChE and suppresse CDC42 and IL6.**

(A) Genotyped sequences of the two AChE alleles in human brain tissues. (B) Similar brain miR-608 levels in homozygous samples of both AChE alleles. (C-D) Elevated AChE but not BChE activity, in brain tissues from minor allele homozygotes. (E-G) Reduced CDC42 and IL6 in brains tissues homozygous for the minor allele.

**Figure 5: Healthy heterozygotes and homozygotes for the minor rs17228616 allele show reduced cortisol, and elevated blood pressure.**

(A) Numbers of homozygotes for the major allele and homozygotes and heterozygotes for the minor rs17228616 allele in the HERITAGE cohort. (B-D) Meta-analysis of different ethnic origins reveals reduced serum cortisol and elevated systolic and diastolic blood pressure in heterozygotes and homozygotes for the minor allele.

**Figure 6: Brain CDC42 inhibition increases anxiety in mice.**

(A) ICV injection of the CDC42 inhibitor ML141 was followed by mouse anxiety and motor functioning tests. (B) ML141 suppresses hippocampal CDC42 GTPase activity. (C-F) ML141-injected mice prefer the periphery over the center in an open field while traveling similar distances. (G-H) ML141-injected mice prefer closed over open elevated plus maze arms. (I) The major AChE allele enables balanced AChE, CDC42 and IL6 levels, which together contribute to controlling anxiety and blood pressure.

The minor AChE allele enhances AChE levels and reduces CDC42 and IL6, thereby dually elevating anxiety and blood pressure.

**Supplementary Figure 1:**

(A) miR-608 is transcribed from intron 3 in the SEMA4G gene, with its promoter-binding transcription factors. (B) Representative miR-608 sequencing product from human intestine and brain. (C-D) Life and death assay of HEK-293T cells carrying AChE 3'UTR fused to cytotoxic sensor. In case of binding to the 3'UTR the cells survive but in lack of binding cells die. (E) Copy number of AChE 3'UTR in stable HEK-293T lines. (F) miR-608 expression in transfected 293T cells with prevalent or SNP AChE 3'UTR. (G) Primers used for site directed mutagenesis to create the minor allele of SNP C2098A AChE 3'UTR sequence. (H) Duplicate SPR experiment of miR-608 binding to major or minor allele of SNP C2098A in AChE.

**Supplementary Figure 2:**

**Healthy heterozygotes and homozygotes of the minor allele of C2098A SNP show elevated cortisol, and blood pressure.**

(A) Numbers of homozygotes for the major allele anf homozygotes and heterozygotes for the minor allele of SNP C2098A in the HERITAGE cohort. (B-C) Elevated serum C-reactive protein and trait, but not state anxiety in in heterozygous and homozygous of the minor allele. (D-E) Distinct distribution patterns of C-reactive protein, trait but not state anxiety, serum cortisol levels and systolic and diastolic blood pressure in heterozygous and homozygous of the minor allele. (F-G) CRP and STAT scores of heterozygous and homozygous to the minor allele compared with homozygous of the major allele.


227x297mm (200 x 200 DPI)

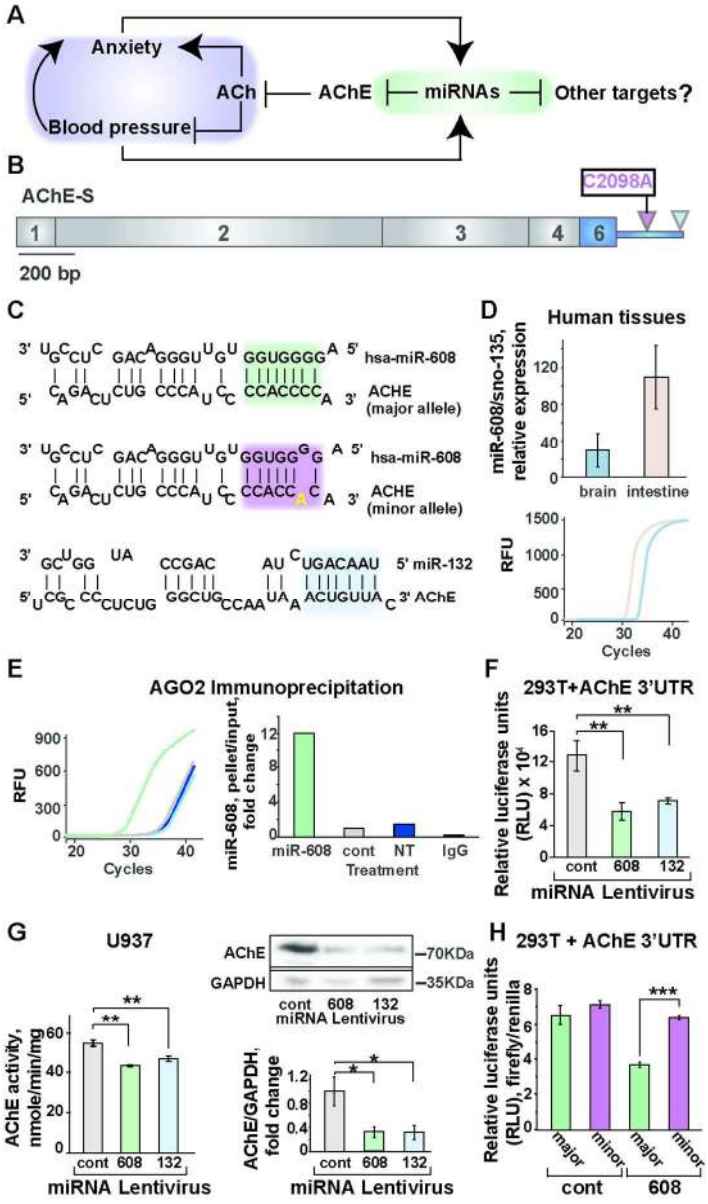


89x152mm (300 x 300 DPI)

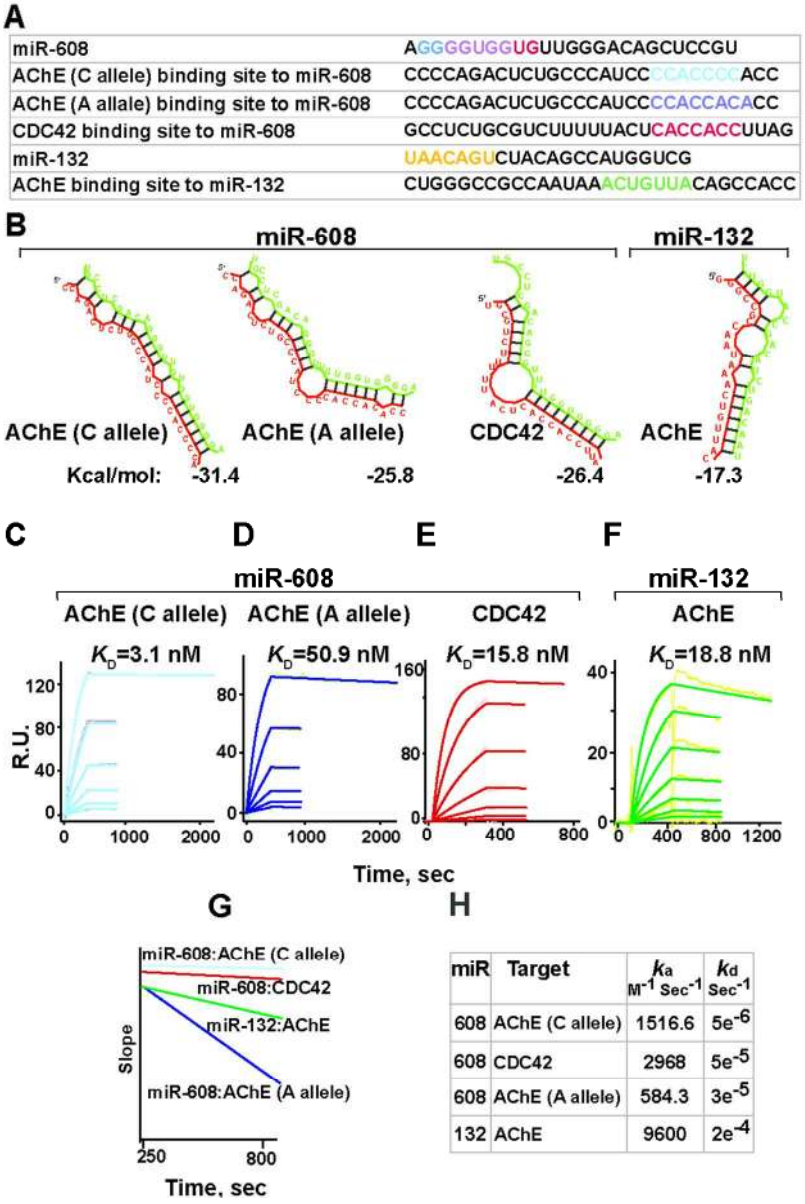


| miR | Target | $k_a$ $M^{-1}$ $Sec^{-1}$ | $k_d$ $Sec^{-1}$ |
|---|---|---|---|
| 608 | AChE (C allele) | 1516.6 | $5e^{-6}$ |
| 608 | CDC42 | 2968 | $5e^{-5}$ |
| 608 | AChE (A allele) | 584.3 | $3e^{-5}$ |
| 132 | AChE | 9600 | $2e^{-4}$ |

89x130mm (300 x 300 DPI)

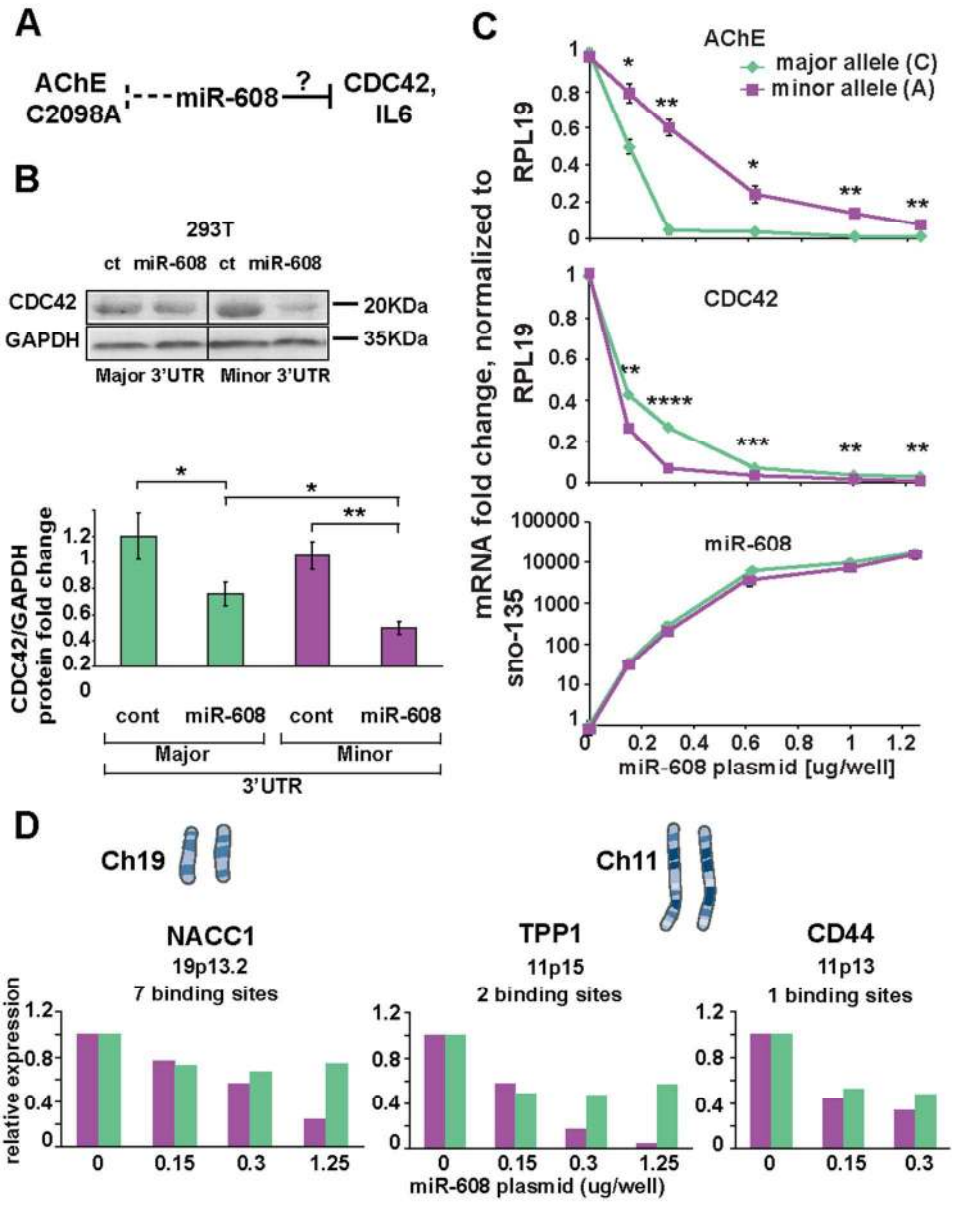


89x112mm (300 x 300 DPI)

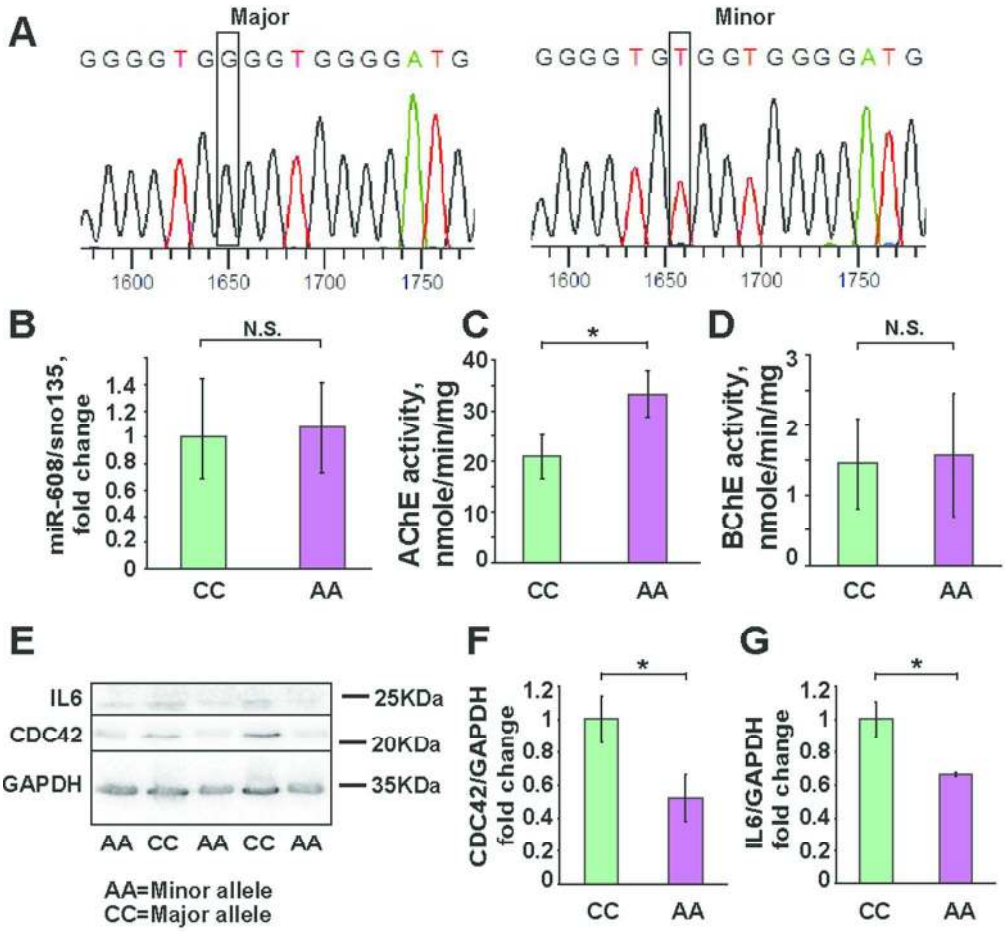


87x81mm (300 x 300 DPI)

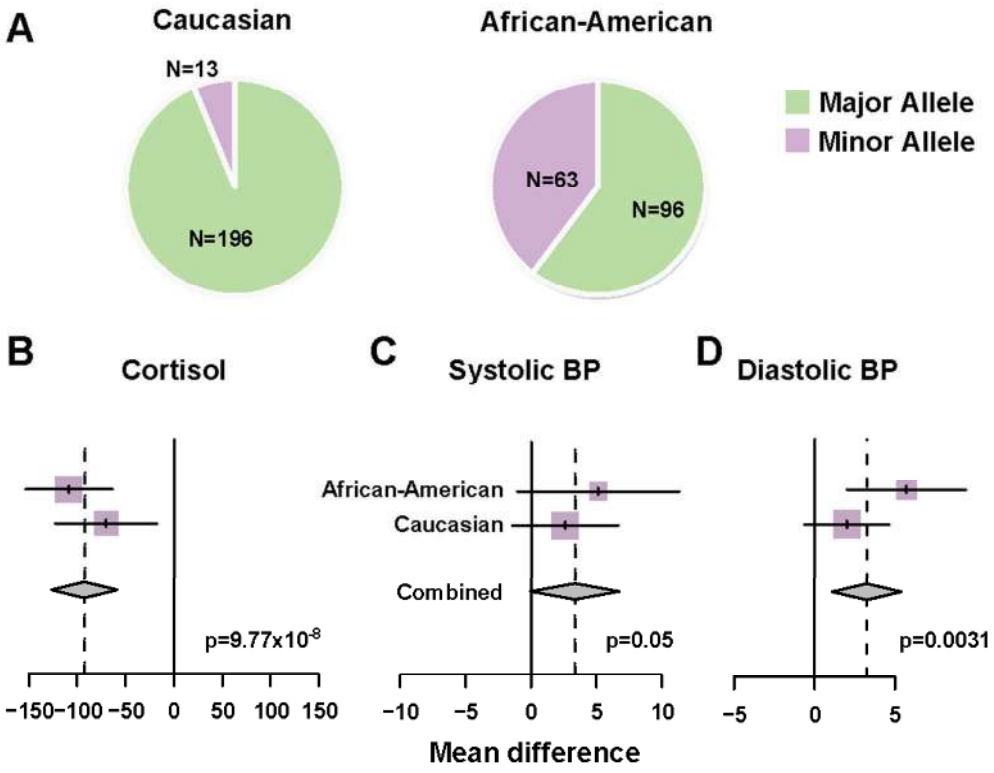


89x69mm (300 x 300 DPI)

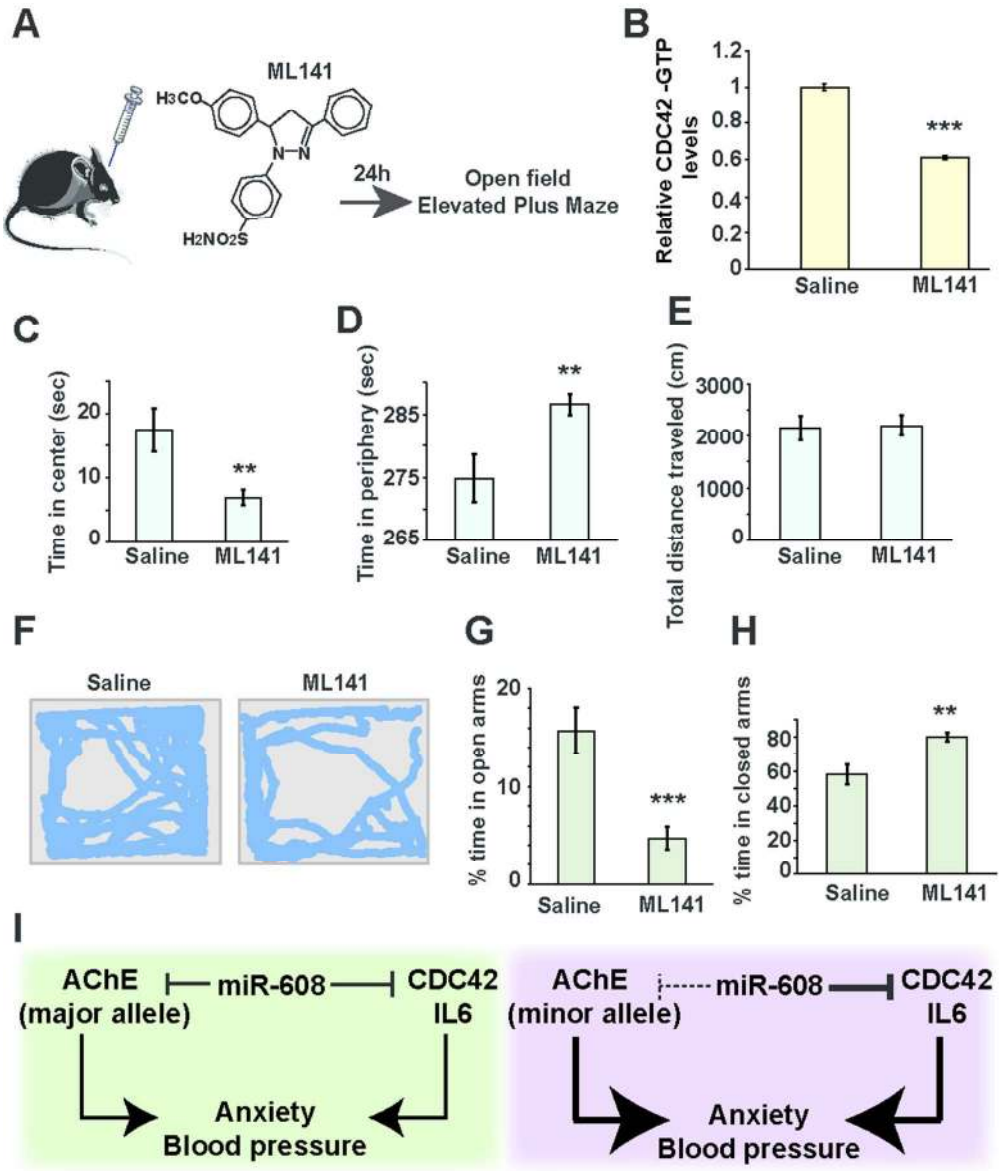


89x104mm (300 x 300 DPI)